iScience

CellPress

Article

Pluripotent Stem Cell-Based Drug Screening Reveals Cardiac Glycosides as Modulators of Myotonic Dystrophy Type 1

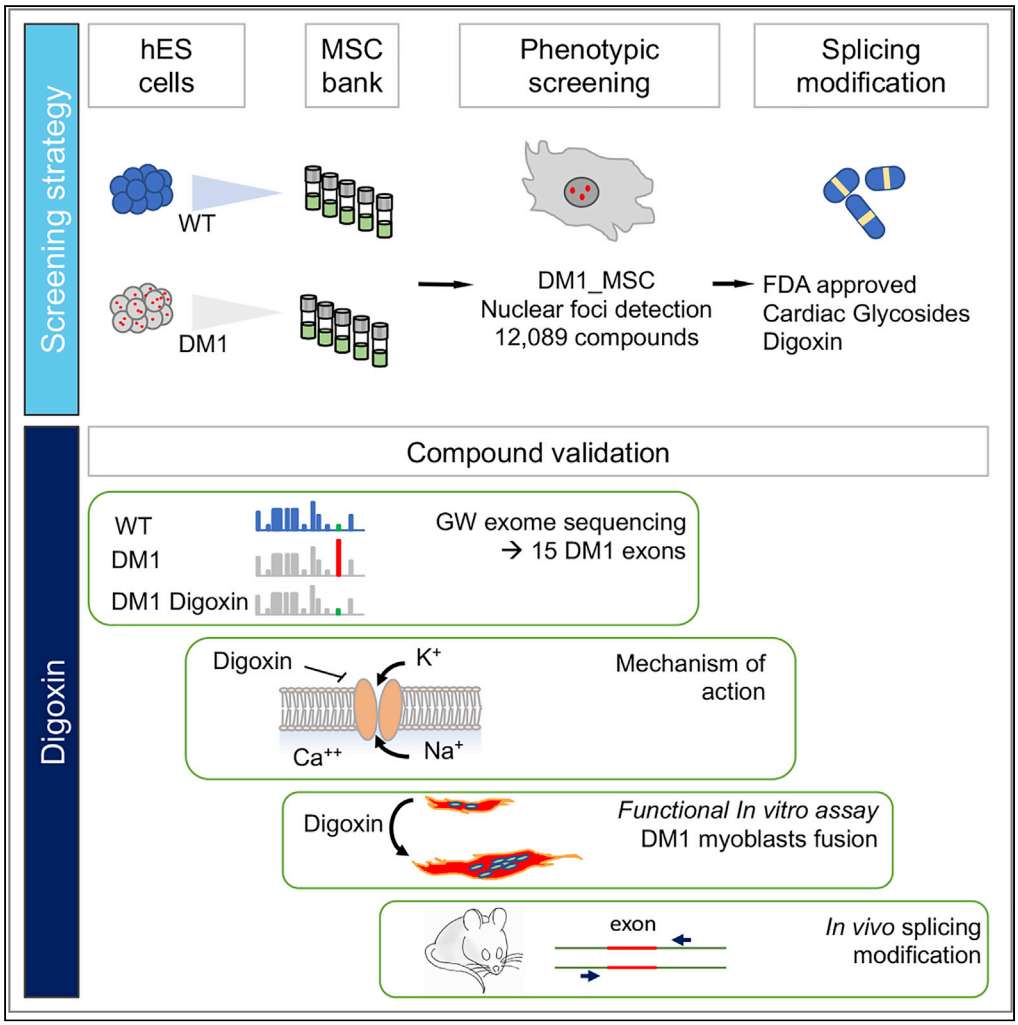

Yves Maury, Pauline Poydenot, Benjamin Brinon, ..., Sandrine Baghdoyan, Marc Peschanski, Cécile Martinat

cmartinat@istem.fr

HIGHLIGHTS

Myotonic dystrophy type 1 hPSCs were adapted for high content screening

FDA-approved cardiac glycosides normalize *in vitro* and *in vivo* DM1 biological markers

Cardiac glycosides synergize with the ERK pathway to normalize DM1 biomarkers

This study emphasizes the value of human pluripotent stem cells for drug discovery

Maury et al., iScience *11*, 258–271
January 25, 2019
https://doi.org/10.1016/j.isci.2018.12.019

iScience

CellPress

Article

Pluripotent Stem Cell-Based Drug Screening Reveals Cardiac Glycosides as Modulators of Myotonic Dystrophy Type 1

Yves Maury,[1] Pauline Poydenot,[1] Benjamin Brinon,[1] Lea Lesueur,[2] Jacqueline Gide,[1] Sylvain Roquevière,[2] Julien Côme,[1] Hélène Polvèche,[3] Didier Auboeuf,[3] Jérome Alexandre Denis,[2] Geneviève Pietu,[2] Denis Furling,[4] Marc Lechuga,[1] Sandrine Baghdoyan,[2] Marc Peschanski,[1,2] and Cécile Martinat[2,5,*]

SUMMARY

There is currently no treatment for myotonic dystrophy type 1 (DM1), the most frequent myopathy of genetic origin. This progressive neuromuscular disease is caused by nuclear-retained RNAs containing expanded CUG repeats. These toxic RNAs alter the activities of RNA splicing factors, resulting in alternative splicing misregulation. By combining human mutated pluripotent stem cells and phenotypic drug screening, we revealed that cardiac glycosides act as modulators for both upstream nuclear aggregations of DMPK mRNAs and several downstream alternative mRNA splicing defects. However, these occurred at different drug concentration ranges. Similar biological effects were recorded in a DM1 mouse model. At the mechanistic level, we demonstrated that this effect was calcium dependent and was synergic with inhibition of the ERK pathway. These results further underscore the value of stem-cell-based assays for drug discovery in monogenic diseases.

INTRODUCTION

Myotonic dystrophy type 1 (DM1) is the most common form of adult muscular dystrophy of genetic origin, with a prevalence of 1/8,000 worldwide, and remains a disease for which there is no treatment. Its multisystemic symptoms, which include myotonia, muscle wasting, cardiac conduction defects, insulin resistance, cataracts, and cognitive dysfunction, are linked to dysregulation and alternative splicing of RNA that affects hundreds of genes (Du et al., 2010; Nakamori et al., 2013; Turner and Hilton-Jones, 2014). The origin of this dysregulation lies in changes to the bioavailability of RNA-binding proteins, in particular MBNL1, which is sequestered in intranuclear ribonucleoprotein aggregates (called foci) and triggered by a CTG repeat expansion in the 3′ UTR of the *DMPK* (dystrophic myotonia protein kinase) gene (Kanadia et al., 2003; Mahadevan et al., 1992). Accordingly, a major ongoing effort aims to generate therapeutic tools that are specifically engineered to target the upstream molecular substrate of the disease by modifying the pathological binding between the mutant mRNA and proteins (Thornton et al., 2017).

A complementary approach to drug discovery has recently been made possible by demonstrating that cells differentiated from pluripotent stem cell lines carrying the mutant *DMPK* gene—obtained as embryonic stem (ES) cell lines from preimplantation genetically diagnosed (PGD) embryos or via reprogramming induced pluripotent stem cell lines from patients—recapitulate major cellular and molecular hallmarks of the disease (Denis et al., 2013; Du et al., 2013; Gauthier et al., 2013; Marteyn et al., 2011; Ueki et al., 2017). These cell lines provide an endless supply of well-characterized biological resources that are amenable to unbiased phenotypic high-throughput drug screening. Over recent years, such an approach has been revealed to be instrumental in identifying candidate therapeutic compounds for other monogenic diseases, such as familial dysautonomia, Huntington disease, Phelan-McDermid syndrome, and progeria (Charbord et al., 2013; Darville et al., 2016; Lee et al., 2012a).

In the current study, we used cells differentiated from an ES cell line, derived from a human embryo carrying a DM1 mutation, to seek compounds that would affect foci and alternative splicing changes. This approach revealed the beneficial effects of US Food and Drug Administration (FDA)-approved cardiac glycosides both on DM1 biological markers and in an *in vitro* myogenic defect as a functional validation of our findings.

[1]CECS, I-STEM, AFM, 91100 Corbeil-Essonnes, France

[2]INSERM, UMR 861, UEVE, ISTEM, AFM, 91100 Corbeil-Essonnes, France

[3]LBMC, 69007 Lyon, France

[4]Sorbonne Universités UPMC Univ Paris 06, INSERM, Centre de Recherche en Myologie - UMRS974, Institut de Myologie, 75013 Paris, France

[5]Lead Contact

*Correspondence: cmartinat@istem.fr

https://doi.org/10.1016/j.isci.2018.12.019

RESULTS

High-Throughput Drug Screening on DM1 Cells

The drug screening workflow involved two sequential steps: (1) a primary assay in which foci were quantified by automated cell imaging, (2) a dose-response exploration of hit compounds for their effects on both foci and selected DM1-specific alternative splicing defects using qRT-PCR. The entire screening process was conducted on mesodermal stem cells (DM1_MSCs), differentiated from an ES cell line derived from a PGD embryo carrying over 1,000 CUG repeats. Screening values were compared with non-treated DM1_MSCs and wild-type (WT)_MSCs that were differentiated from an unaffected ES cell line (Marteyn et al., 2011). Results were secondarily validated in other cell and animal models for the disease.

Nuclear foci were identified in DM1_MSCs using an automated RNA fluorescence *in situ* hybridization assay that was developed to detect expanded CUG repeats (Figure S1A). DM1_MSCs contained an average of 2.5 foci, whereas none were observed in control cells (Figure 1A). Results were confirmed as robust based on a high Z-factor, of 0.71, calculated for the assay (Figure 1B).

The primary drug screening was carried out by considering the number of intranuclear foci per cell using 12,089 compounds assayed at a concentration of 10 μM, including a set of 1,120 FDA-approved drugs. Compounds were selected as candidates when the number of foci reached 1.5 standard deviations below the mean value for untreated DM1_MSCs, in the absence of unacceptable cytotoxicity (cutoff for cell survival set at 20% of control). This target was then revealed as non-informative, because none of the compounds that were tested demonstrated a capacity for decreasing the number of foci in the absence of unacceptable cell toxicity. Four hit compounds only emerged once these results were secondarily filtered by taking into account the average area of individual intranuclear foci. Their effects were characterized by an increased number of foci per nuclei in conjunction with their size reduction, which suggested a partial disaggregation of ribonucleoprotein inclusions. These compounds were cycloheximide (CHX) and three members of the cardiac glycoside family, namely, strophantidin, ouabain, and digoxigenin (Figures 1C and S1B). The first compound, CHX, was excluded from further analysis owing to its well-known activity as a protein synthesis inhibitor. In support of the hypothesis that the apparent reduction in size of the foci was due to a general decrease in cell protein content, we observed a decreased expression of MBNL1 and CUGBP1, as well as an exacerbation of defective alternative splicing associated with DM1 after treatment with CHX (Figure S2). The identification of three cardiac glycosides in the screening campaign suggested a common mechanism of action, and four additional members of this chemical family were therefore included in dose-response experiments, revealing similar dose-dependent effects: an increased number of foci per nucleus associated with a size reduction of each focus (Figures 1D and 1E).

In parallel, a concomitant rescue of dysregulated alternative splicing was sought using the defective inclusion of exon 11 in the insulin receptor (*IR*) gene that was described as a representative in DM1 (Savkur et al., 2001) (Figure 2A). The ratio of IRB (containing exon 11) to IRA (excluding exon 11) was used as a readout. Although the action of cardiac glycosides on the foci parameters was efficient at the micromolar range, it was associated with decreased cell viability, as well as an exacerbation of the DM1-related IR splicing defect, decreasing the ratio of *IR* transcripts. Conversely, all cardiac glycosides that were tested normalized the DM1-altered ratio of *IR* transcripts at concentrations ranging from 10 nM to 500 nM, depending on the chemical structure, in the absence of overt cytotoxicity and of any effect on foci (Figures 2B and 2C).

Digoxin Effect on Alternative mRNA Splicing

Digoxin, the best documented and most commonly prescribed medication in the cardiac glycoside family, was used as a representative to further characterize the therapeutic potential in DM1.

The long-term effect of this drug was demonstrated by chronic treatment of DM1_MSCs with 50 nM digoxin for 4 weeks in standard tissue culture T75 flasks, with analysis of one sample at each time point. This treatment induced a stable splicing switch of the *IR* exon 11 and *SERCA1* exon 22 from a DM1 to a WT pattern (Figure 3A). This effect was observed in the absence of a concomitant effect of the treatment on the number and size of the foci. Other splice defects associated with DM1 were also shown to be normalized, including *cTNT* exon 5, *CLCN*-1 exon 7a in DM1_hES-derived MSCs, and *NMDAR1* exon 5 in DM1_hES-derived neurons after a 48-hr treatment period (Figure S3).

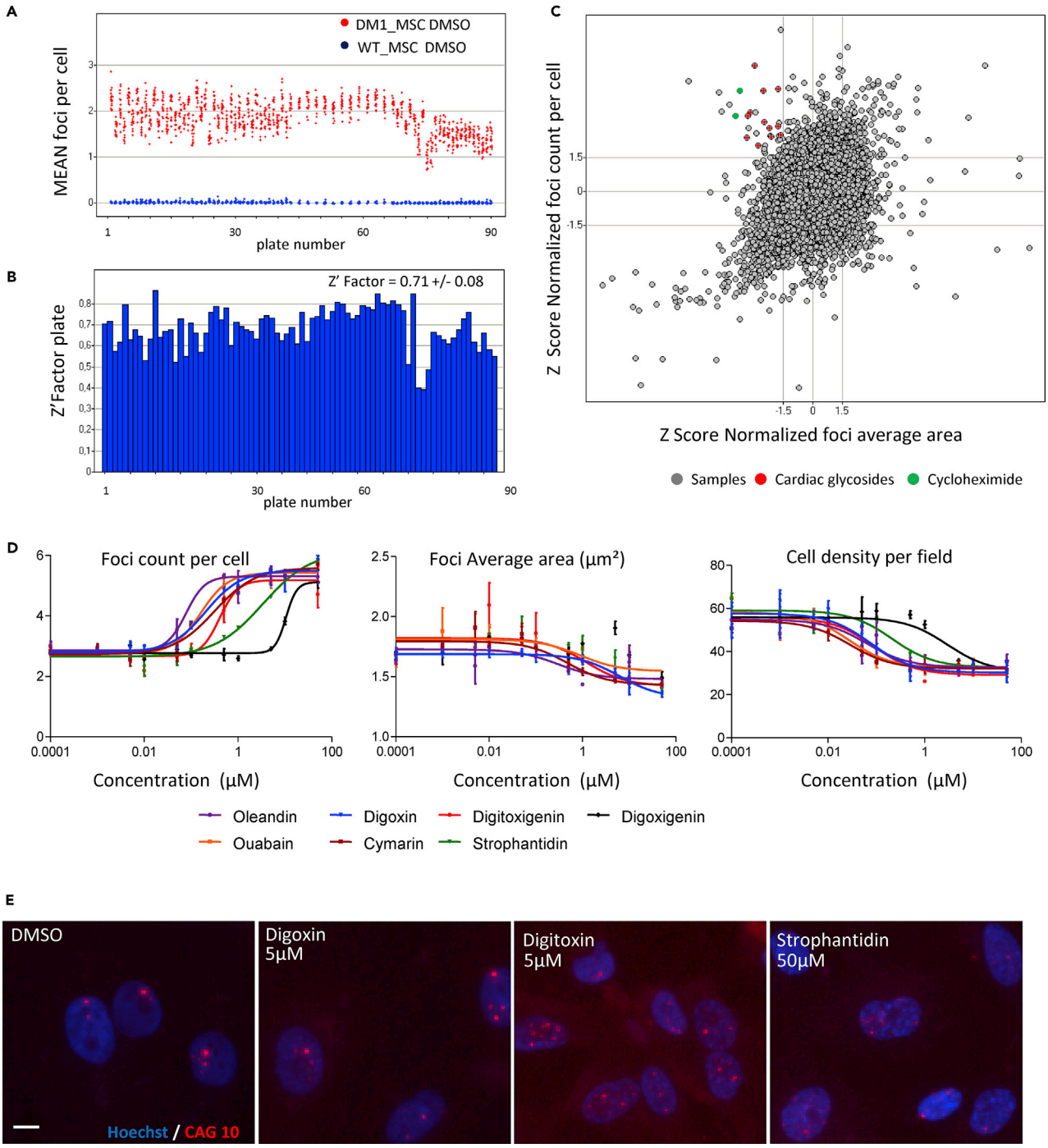

Figure 1. Development of a High-Content Assay for Mutant DMPK Foci

(A) Mean number of detected foci per cell in untreated DM1-MSCs (red dots) and WT_MSCs (blue dots). Each dot represents one well in 90 screening plates.

(B) Determination of the Z′ factor by using the number of detected foci per cell between DM1 and WT_MSCs for each plate, with a mean value of around 0.7 for the whole screening campaign.

(C) Scatterplot representation of the primary screening analysis based on the number of detected foci per cell and average area of foci after normalization in non-treated DM1_MSCs. Validated compounds are shown with colored dots.

(D) Dose-response analysis for number of foci, area of foci, and cell density in DM1_MSCs after 48 hr treatment with seven cardiac glycosides. Mean values ± SD are given (10 points in dose-response curve, each in triplicate).

(E) Representative images of mutant DMPK mRNA foci detected by RNA-fluorescence *in situ* hybridization in DM1_MSCs after treatment with three different cardiac glycosides for 48 hr. Scale bar indicates 10 µm.

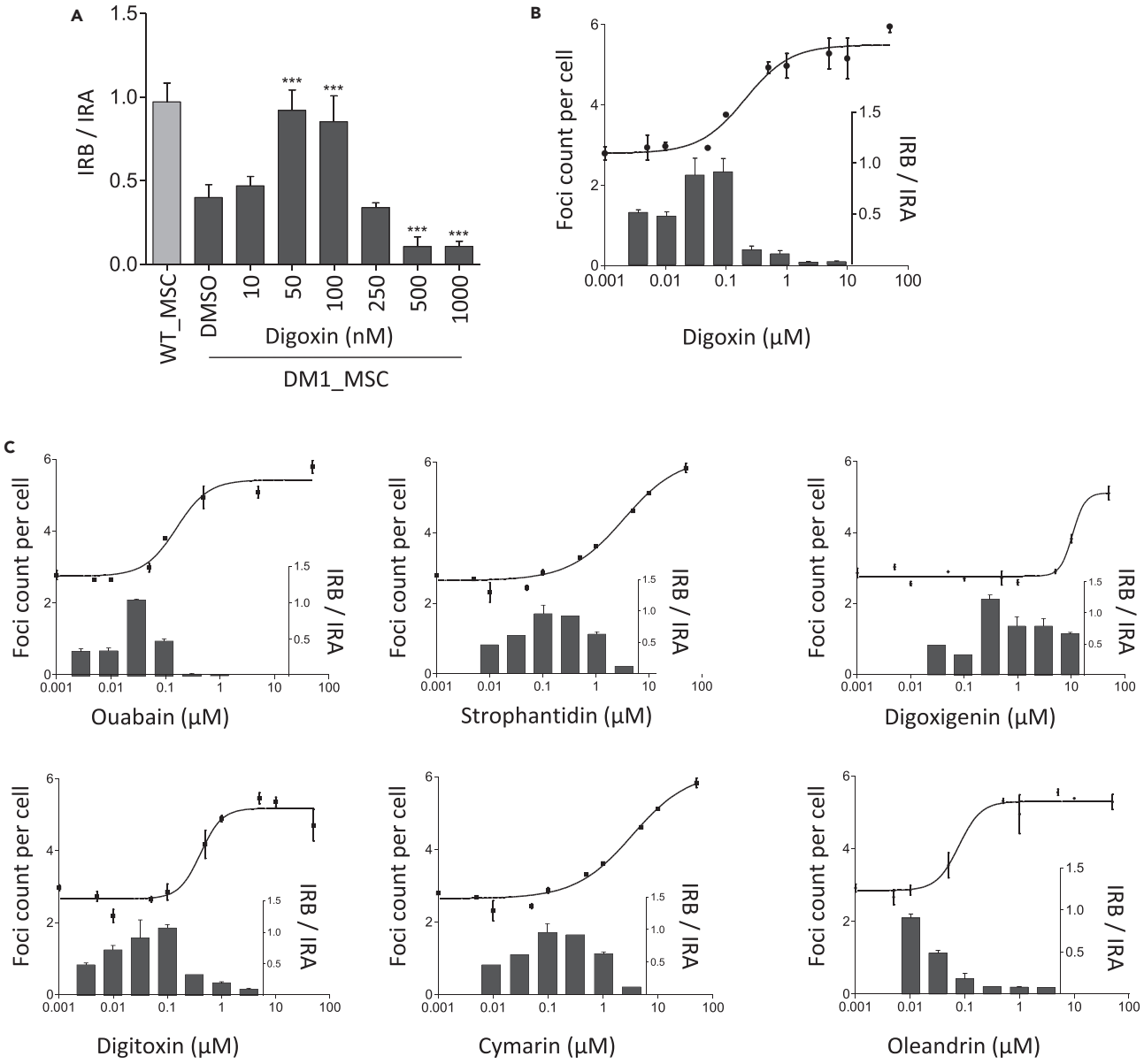

Figure 2. Digoxin Treatment in the Nanomolar Range Rescues Alternative IR and SERCA1 Splicing in DM1 Cells

(A) Dose-response analysis for alternative *IR* splicing in DM1_MSCs treated with digoxin for 48 hr. Relative expression level of the two isoforms of *IR* (IRA [-exon 11] and IRB [+exon 11]) were measured by quantitative real-time RT-PCR. Data represent the ratio of *IRB*/*IRA* and are indicated as mean ± SD (n = 3). Data were analyzed with one way ANOVA, followed by a Dunnett post-hoc test. ***: p-value < 0.001.

(B) Superposition of the concentration-dependent effect of digoxin on the number of foci per cell (solid line, left axis) and alternative *IR* splicing (black bars, right axis) on DM1_MSCs treated for 48 hr.

(C) Dose-response analysis of six different cardiac glycosides on mutant DMPK foci (solid lines; n = 2; mean ± SEM) and alternative *IR* splicing (bars; n = 2, mean ± SD) in DM1_MSCs treated for 48 hr.

The ability of cardiac glycosides to modulate RNA processing independently of an effect on foci was confirmed by treating WT_MSCs with nanomolar digoxin concentrations. This also led to an increased inclusion of exon 11 in *IR* and exon 22 in *SERCA1* in these cells, although above control values in these cases (Figures 3B and 3C). Similar results were obtained with other cellular systems, namely, primary cultures of myoblasts and human embryonic stem cells (hES)-derived neurons (Figures 3D and S3C). In addition, there was no effect of digoxin, either on the level of expression or on the localization of MBNL1 and CUGBP1 in DM1 cells, the mislocalization and change in bioavailability of which are deemed responsible for the

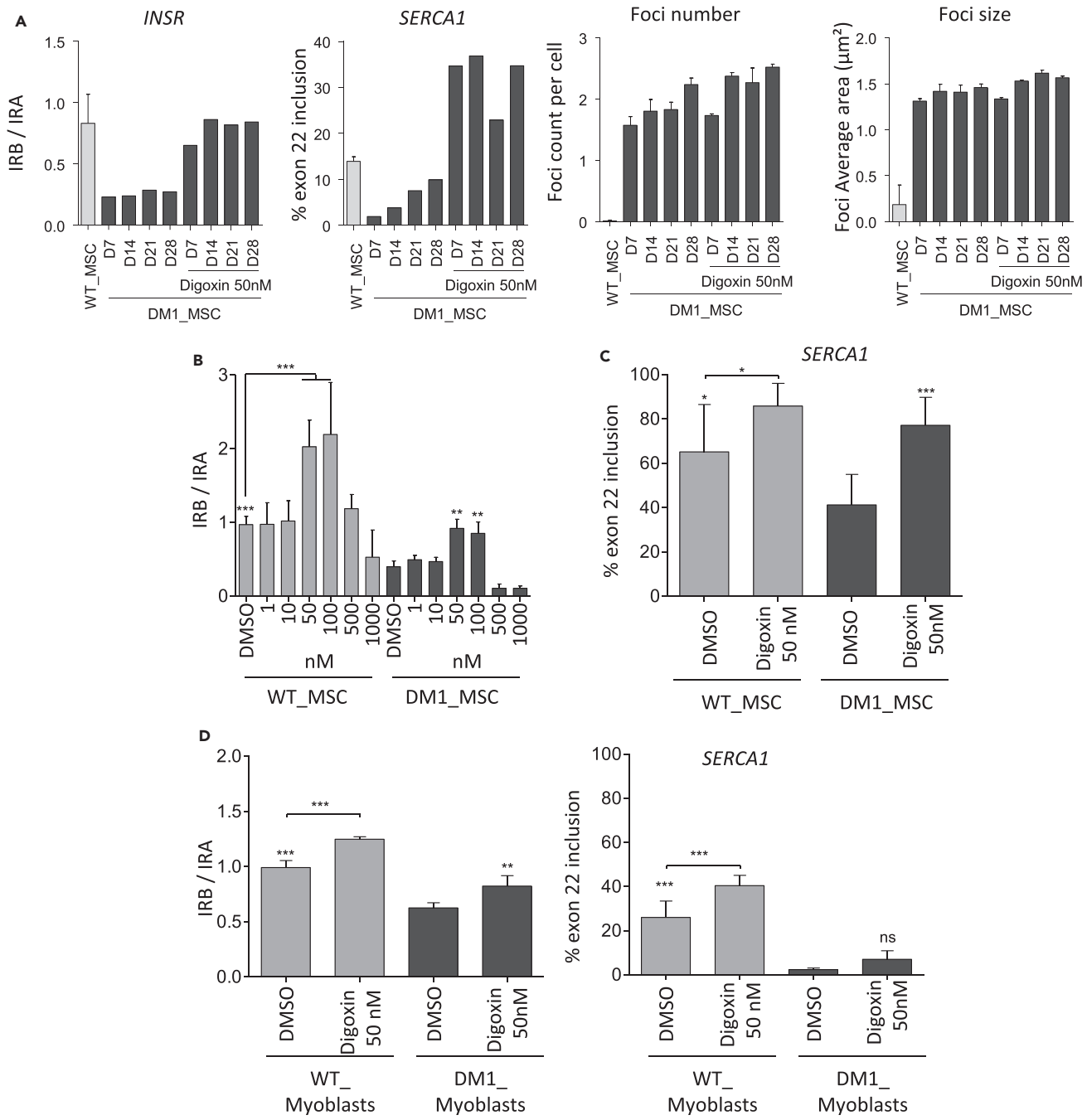

Figure 3. Digoxin Treatment Rescues Alternative *IR* and *SERCA1* Splicing in DM1 Cells

(A) Effect of chronic digoxin treatment on mutant DMPK foci and alternative splicing of IR and SERCA1. DM1_MSCs were continuously treated with 50 nM of digoxin over 4 weeks. Mutant DMPK foci and alternative splicing of *IR* and *SERCA1* were analyzed every 7 days. Untreated WT_MSCs were used as the control. For alternative *IR* and *SERCA1* splicing, one sample was analyzed at each time point. Relative expression levels of the two isoforms of *IR* (*IRA* [-exon 11] and *IRB* [+exon 11]) were measured by real-time quantitative RT-PCR. Data represent the ratio of *IRB*/*IRA* (n = 1 at each time point). Alternative *IR* splicing was analyzed using real-time quantitative RT-PCR. The percentage for inclusion of *SERCA1* exon 22 was determined by RT-PCR, followed by analysis with a 2100 Bioanalyzer (Agilent). Quantification of each band was performed using 2100 Expert software. For mutant DMPK foci, data are presented as mean ± SD (n = 4).

(B) Concentration-dependent effect of digoxin on alternative *IR* splicing in WT and DM1_MSCs. Relative expression levels of the two isoforms of *IRA* [-exon 11] and *IRB* [+exon 11]) were measured by real-time quantitative RT-PCR. Data represent the ratio of *IRB*/*IRA*.

(C) Effect of digoxin treatment at 50 nM for 48 hr on the inclusion of exon 22 of *SERCA1* in WT and DM1_MSCs, determined by RT-PCR, followed by analysis with a 2100 Bioanalyzer (Agilent).

Figure 3. *Continued*

(D) Effect of digoxin treatment on alternative *IR* and *SERCA1* splicing in primary myoblasts isolated from healthy individuals and patients with DM1.

For all graphs, data are presented as mean ± SD (n = 3) and analyzed with one-way ANOVA, followed by a Bonferroni post-hoc test. *p < 0.05, **p < 0.01, ***p < 0.001.

impairment of alternative mRNA splicing (Figures S4A–S4C and S4E). The consequences of digoxin treatment on alternative mRNA splicing were thus explored more comprehensively using deep RNA sequencing, comparing DM1_MSCs with or without treatment with 50 nM of the drug over a period of 2 days. Analysis of annotated splice junctions identified 44 modified splices with Delta $\psi \geq 20$ and 258 with $10 \leq$ Delta $\psi \leq 20$ (Tables S1 and S2). The comparison of this dataset with a recently published list of genes, which exhibited dysregulated alternative RNA splicing in muscle biopsies from patients with DM1 (Nakamori et al., 2013), revealed a beneficial effect of digoxin treatment on 10 different DM1-specific splicing defects as determined by qRT-PCR analysis (Figure 4).

Finally, the effect of digoxin was evaluated *in vivo*, in the HSA^{LR} transgenic DM1 mouse model, which expresses 220 CUG repeats in skeletal muscle and exhibits dysregulated alternative splicing (Mankodi et al., 2002). Digoxin was administrated daily by intraperitoneal injection for 7 days at two dosage regimens: 0.02mg/kg and 2 mg/kg/ d. Rescue of *Mbnl1-, Ldb3-,* and *Clcn1*-dysregulated RNA splicing was observed after digoxin treatment at the lower dosage (Figures 5A and S5), independent of any changes in expression of the HSA transgene (Figure 5B). Mbnl1 exon 5 inclusion, for instance, was recorded at 17.44% ± 2.7% after digoxin treatment at 0.02mg/kg/d, down from 35.13% ± 2.2% in untreated HSA^{LR} mice (FigureS5).

Molecular Mechanisms that Underlie the Effects of Cardiac Glycosides on Alternative RNA Splicing

A series of hypotheses were sequentially explored in a search for the molecular mechanisms underlying the potential therapeutic effects of cardiac glycosides.

We first checked whether these effects were associated with a change in the intracellular concentration of calcium, which is the common outcome of treatments with cardiac glycosides. To this end, we used the calcium ionophore A23187, which increases intracellular calcium content (Dedkova et al., 2000). Treatment with the calcium ionophore A23187 had a similar effect on the *IR* splicing ratio as that produced by digoxin. A combination of digoxin and A23187 led to neither an additive nor a synergistic effect (Figure 6A), supporting the hypothesis of a calcium-dependent mechanism for digoxin effects on alternative mRNA splicing. This was further validated by the abolition of the drug effect on alternative *IR* and *SERCA1* splicing when calcium was withdrawn from the cell culture medium (Figures 6B and 6C).

The next step in the analysis aimed at determining intracellular signaling pathways that may be triggered by the drug and that may affect alternative splicing. Cardiac glycosides are sodium-potassium pump inhibitors that activate multiple cell signaling pathways, representing many other possible mechanisms by which these compounds might affect alternative splicing. Following treatment of DM1_MSCs with 50 or 100 nM digoxin for 48 hr, western blot analyses indicated a moderately increased phosphorylation of AKT and GSK3-β and a decreased activation of ERK (Figure 6D). A combination of digoxin with either LY294002 or CHIR99021, which specifically inhibit AKT and GSK3, respectively, attenuated the beneficial effect of digoxin on *IR* exon 11 inclusion (Figure 6A), indicating that these pathways contribute toward the effects of the drug. Conversely, inhibition of ERK phosphorylation by PD0325901 in DM1_MSC-normalized *IR* exon 11 inclusion in the absence of digoxin, and co-treatment with digoxin, resulted in an additive or synergistic effect, suggesting a cooperative mode of action (Figure 6A). Finally, two RNA-binding proteins that were previously shown to be modulated by cardiac glycosides (Anderson et al., 2012), namely, SRSF3 (SRp20) and TRA2B, were investigated. Western blot analysis revealed that their expression levels were not modified in treated DM1_MSCs (Figures S4D and S4E).

Functional Effects of Digoxin on Myogenic Differentiation

In an attempt to identify a functional correlate for these biological results, the digoxin effect was challenged on DM1 primary human myoblast cells carrying 2000 CTG repeats and displaying defective myotube differentiation *in vitro* (Bigot et al., 2009; Thornell et al., 2009). Digoxin treatment at 50 nM for 7 days increased the number of myotubes that were formed, as quantified by both myosin heavy chain immunostaining (number of MF20-positive cells), and the number of nuclei per MF20-positive cell

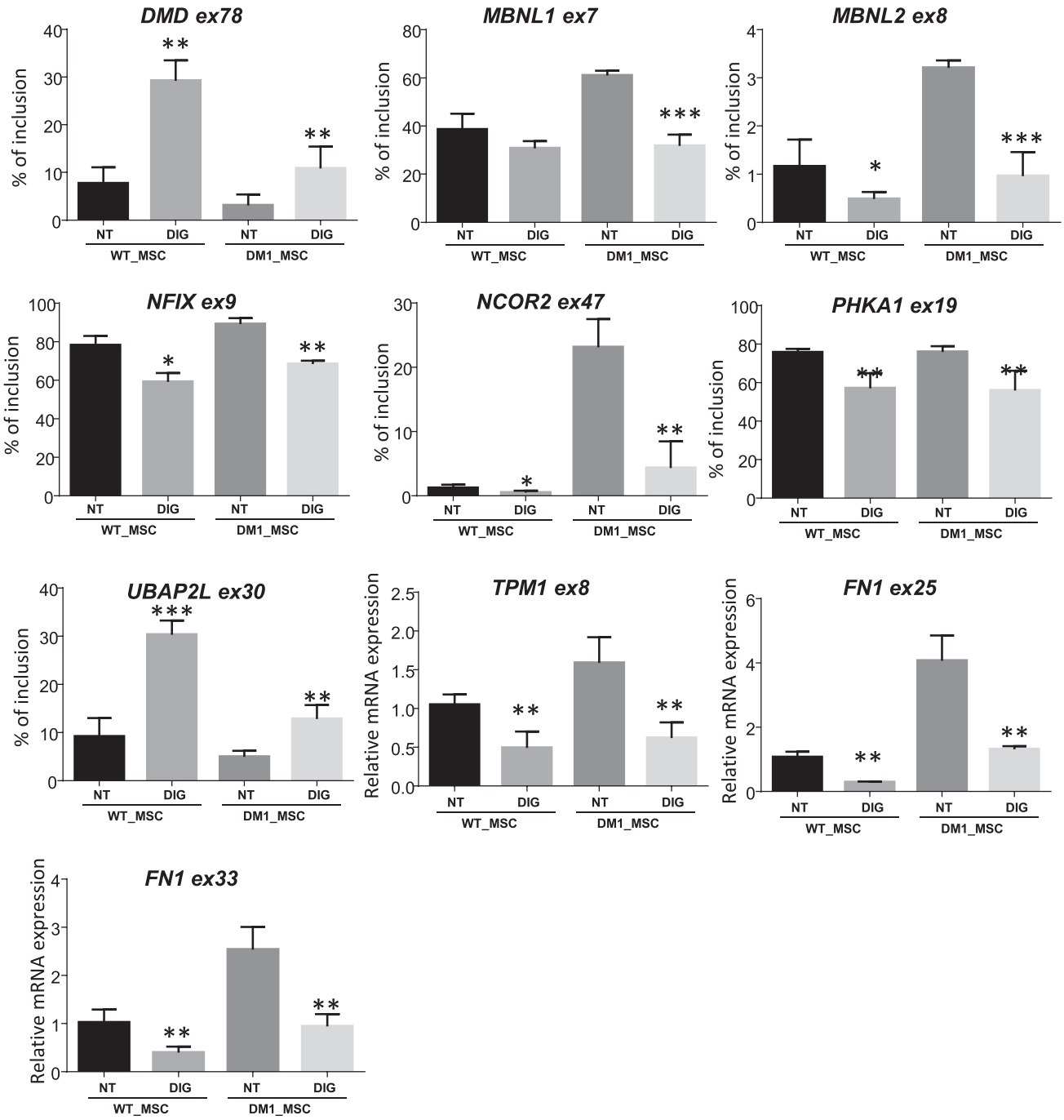

Figure 4. Beneficial Effect of Digoxin Treatment in the Nanomolar Range on Other Alternative Splicing Associated with DM1

RT-PCR analysis of 10 forms of alternative splicing reported to be affected in patients with DM1 and rescued by digoxin treatment (50 nM for 48 hr) in WT and DM1_MSCs. The percentage for inclusion of isoform was determined by RT-PCR, followed by analysis with a 2100 Bioanalyzer (Agilent). Quantification of each band was performed using 2100 Expert software. Data are presented as mean ± SD (n = 3). Data were analyzed with one-way ANOVA, followed by a Dunnett post-hoc test. *$p < 0.05$, **$p < 0.01$, ***$p < 0.001$.

(Figures 7A and 7B and S6). Calcium deprivation in the culture medium during myotube differentiation fully abolished the functional benefit of digoxin treatment (Figure 7C). Similar positive results on the myogenic process were obtained by applying a 50 nM digoxin pulse for the first two days of myoblast differentiation. This observation was further confirmed using other cardiac glycosides (Figure S7). In addition, qRT-PCR

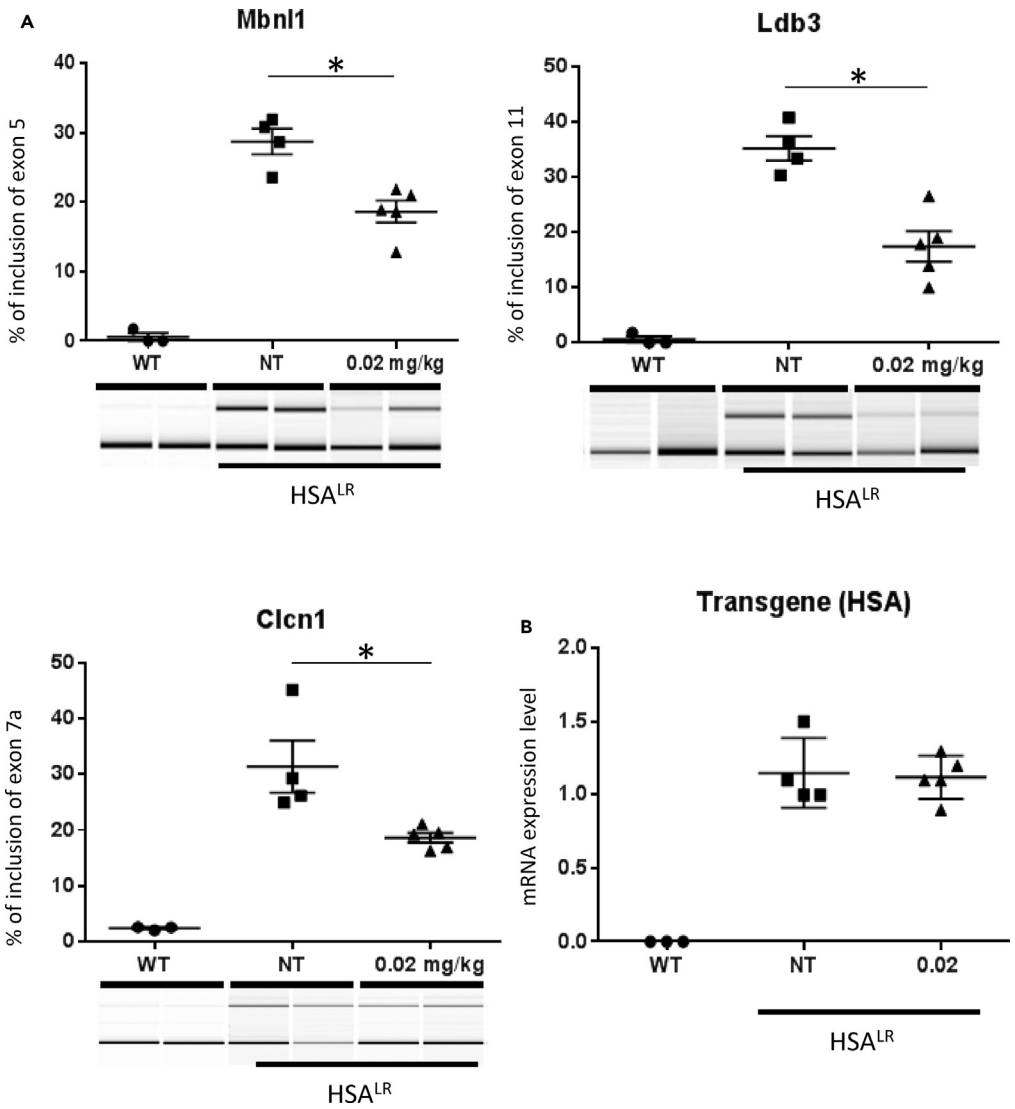

Figure 5. Digoxin Treatment Partially Restores *In Vivo* Splicing Defects in a DM1 Mouse Model

(A) Analysis of *Mbnl1*, *Ldb3*, *Clcn1* alternative splicing by RT-PCR in HSA^{LR} mice treated with intraperitoneal injection of digoxin for 7 days (n = 3 for wild-type, n = 4 for mock-treated, and n = 5 for treated). RT-PCR was followed by analysis with a 2100 Bioanalyzer (Agilent). Quantification of each band was performed using 2100 Expert software. Data are presented as mean ± SEM. The p value was determined using the Mann-Whitney U test; *$p < 0.05$.

(B) Quantitative real-time qRT-PCR analysis of HSA transgene as a function of digoxin treatment. Data were normalized with the housekeeping gene 18S.

analysis of alternate splicing variants revealed a normalization of MBNL1 exon 7, INSR exon 11, and DMD exon 78 in myotubes treated with 50 nM digoxin.

DISCUSSION

The main outcome of this study is the identification of the cardiac glycoside chemical family as constituting a potential therapeutic strategy for DM1. These compounds had the capacity to promote changes toward normalization in alternative mRNA splicing of genes affected by the DM1 mutation and myogenic fusion of affected myoblasts. These results were obtained using high-throughput drug screening, based on human pluripotent stem cell line derivatives that carried the mutant gene and recapitulated the cardinal cellular features of the disease. Similar experimental paradigms may be proposed for a vast array of monogenic diseases as these cellular models give access to relevant readouts.

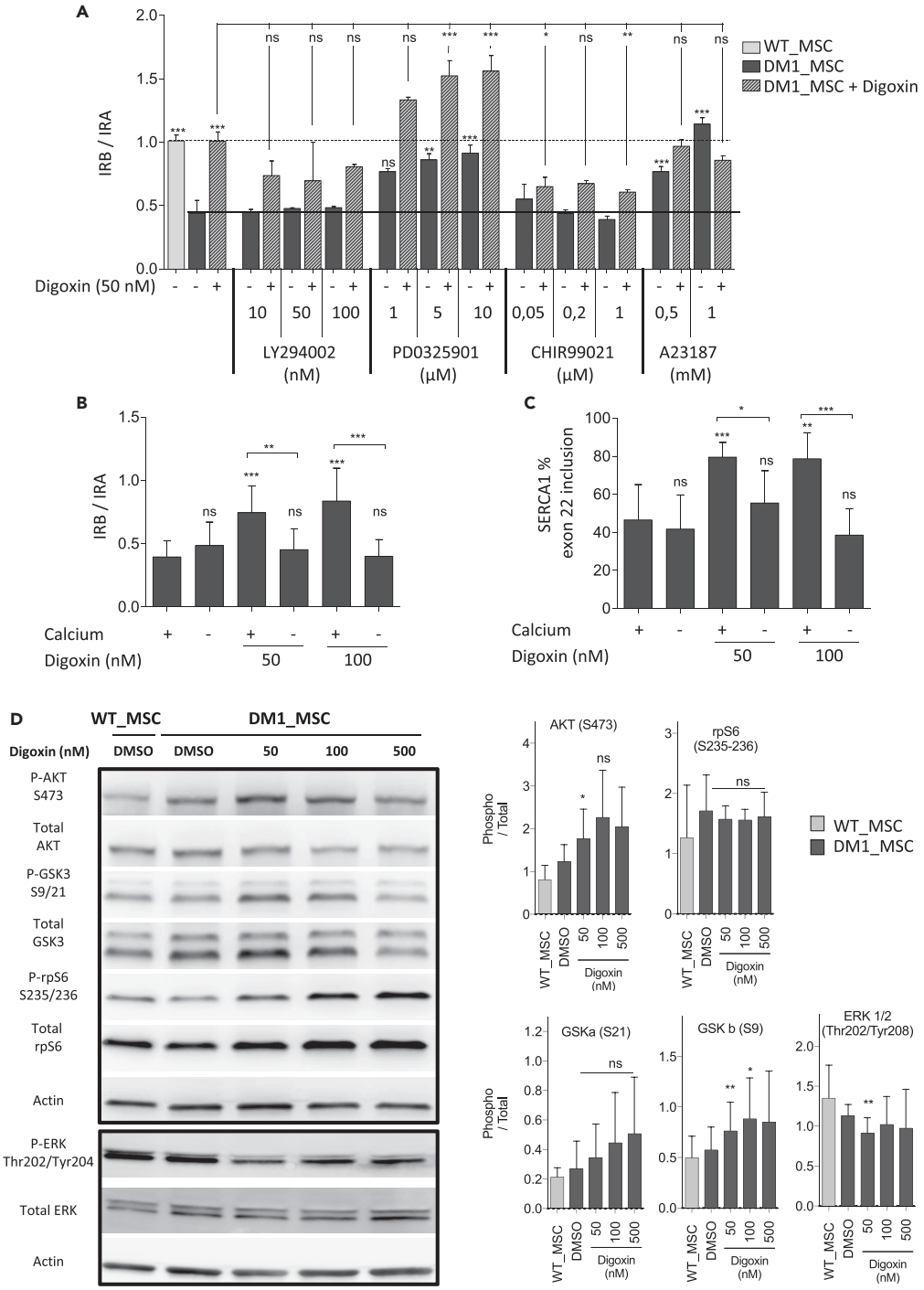

Figure 6. Calcium-Dependent Effect of Digoxin on Alternative Splicing of IR and SERCA1

(A) Pharmacological approaches to analyze the combinatorial effect of AKT, GSK3, ERK, and calcium pathways with digoxin on alternative *IR* splicing. DM1_MSCs were treated for 48 hr, with or without 50 nM of digoxin, in combination with different concentrations of AKT inhibitor (LY29002), GSK3 inhibitor (CHIR99021), ERK inhibitor (PD0325901), or calcium ionophore (A23187). WT_MSCs were used as a positive control. Alternative *IR* splicing was quantified using qRT-PCR. Data are presented as mean ± SD (n = 3).

(B and C) Influence of calcium on the digoxin-mediated effect on alternative splicing of *IR* (B) and SERCA1 (C) in DM1_MSCs. Cells were maintained in medium with or without calcium and treated with digoxin (50 or 100 nM) for 48 hr.

Figure 6. *Continued*

Medium without calcium was added 30 min before the digoxin (n = 3). Data were analyzed with one-way ANOVA followed by a Bonferroni post-hoc test. *p < 0.05, **p < 0.01, ***p < 0.001.

(D) Effect of different concentrations of digoxin on mitogen-activated protein kinase and mammalian target of rapamycin (mTOR) signaling pathways. Expression level of key modulators of Akt/mTOR signaling in DM1_MSCs treated with different concentrations of digoxin for 48 hr, including Phospho(Ser473)-Akt, Phospho(Ser21/9)-GSK3α/β, Phospho(Ser235-236)-ribosomal protein S6 (rpS6), Phospho (Thr202/Tyr204) ERK, and the corresponding total forms. Antibodies used are liste in Table S3. Western blot analysis was quantified by using ImageJ software. Data are presented as mean ± SD (n = 4) and p value were determined using paired t test. *p < 0.05, **p < 0.01.

DM1 is characterized by the accumulation of the mutant DMPK mRNA in cell nuclei, due to the presence of an abnormal tract of CTG triplet repeats in the 3′ UTR of the DMPK gene. This mutation provokes a major alteration in the bioavailability or activity of RNA-binding proteins, most particularly MBNL1 and CUGBP1, in part through the formation of intranuclearribonucleoprotein aggregates (Mankodi et al., 2001). This, in turn, induces changes in alternative RNA splicing in a number of genes that are physiological targets of those proteins. In the present study, cardiac glycosides were shown to affect these pathological mechanisms in different ways, depending upon their concentration. At high cytotoxic concentrations—in the micromolar range—they provoked a partial disaggregation of the inclusions. This, however, did not correlate with a normalization of the alternative RNA splicing activity, which rather deteriorated further as a consequence of cellular toxicity. Such a phenomenon was reminiscent of what was observed in a previous study in which the expression of MBNL1 was decreased in primary fibroblasts derived from patients with DM1 using a specific small interfering RNA (Childs-Disney et al., 2013).

The large variety of alternate splicing defects observed in DM1 are thought to be responsible for the multisystemic nature of this disease, and some reports have already linked the alteration of single mRNA variants to specific disease phenotypes. For instance, the increased inclusion of CLC1 exon 7a is involved in the onset of myotonia, and repression of this exon inclusion using morpholino antisense oligonucleotide greatly reduced the myotonic grade observed in genetic DM1 mouse models (Wheeler et al., 2007). Therefore normalization of abnormal ratios of these transcripts, if obtained under treatment, is expected to be therapeutically relevant. The effects of cardiac glycosides do not, however, specifically target the causative molecular defect of the disease and the extent of the success of treatment for different disease phenotypes can only be partial. Whether the partial recovery of ratios might be therapeutically relevant will need to be explored in a clinical setting. Nevertheless, the positive effect of digoxin recorded in the present study on a myogenesis assay indicates that cardiac glycosides might have functional consequences. These compounds are still regularly prescribed for the management of atrial fibrillation and heart failure in the general population, although their clinical use has been steadily decreasing because of their narrow therapeutic window, which makes them a toxicity risk (Kanji and MacLean, 2012). Given that cardiac conduction abnormalities are critical symptoms in DM1, careful consideration of the indication and cautious observation will be required for administration, as well as close monitoring of the side effects of cardiac glycosides in patients with DM1. However, there are already reports on several patients with DM1 exhibiting good tolerance to digoxin or digitoxin (Finsterer and Stollberger, 2012; LagoeiroJorge et al., 2012; Phillips and Harper, 1997; Schmitt and Schmidt, 1975). It is also notable that the narrow concentration range in which digoxin exerts a beneficial effect on DM1 phenotypes in this study is similar to tissue concentrations found in patients treated for heart failure (Hothi et al., 2014; Schoner and Scheiner-Bobis, 2007).

The ultimate goal of a DM1 therapy is the correction of all affected genes. Targeting the causative mechanisms of the pathology, at the level of either the DMPK gene mutation or by introducing competition to its mRNA binding to splicing factors such as MBNL1, would obviously be the most elegant therapy. This is being actively pursued by a number of teams who have developed various approaches based on gene transfer, antisense oligonucleotides, or specific synthetic small molecules (Childs-Disney et al., 2012, 2013; Francois et al., 2011; Ketley et al., 2013; Laustriat et al., 2015; Lee et al., 2012b; Mulders et al., 2009; Nakamori et al., 2016; Pandey et al., 2015; Parkesh et al., 2012; Wheeler et al., 2012). Current results point to a parallel pharmacological approach, aiming at modifying alternative RNA splicing of as many DM1-affected genes as possible, without affecting the causative mechanisms of the disease. Such an approach would benefit from a combination of drugs. Indeed, cardiac glycosides are not an isolated case. Two small molecules have recently been clinically evaluated in DM1: the anti-myotonic mexiletine (Logigian et al., 2010) and, more recently, the anti-diabetic drug metformin (Laustriat et al., 2015). Interestingly, the mechanism of action for cardiac glyocosides differs from that for these previously mentioned

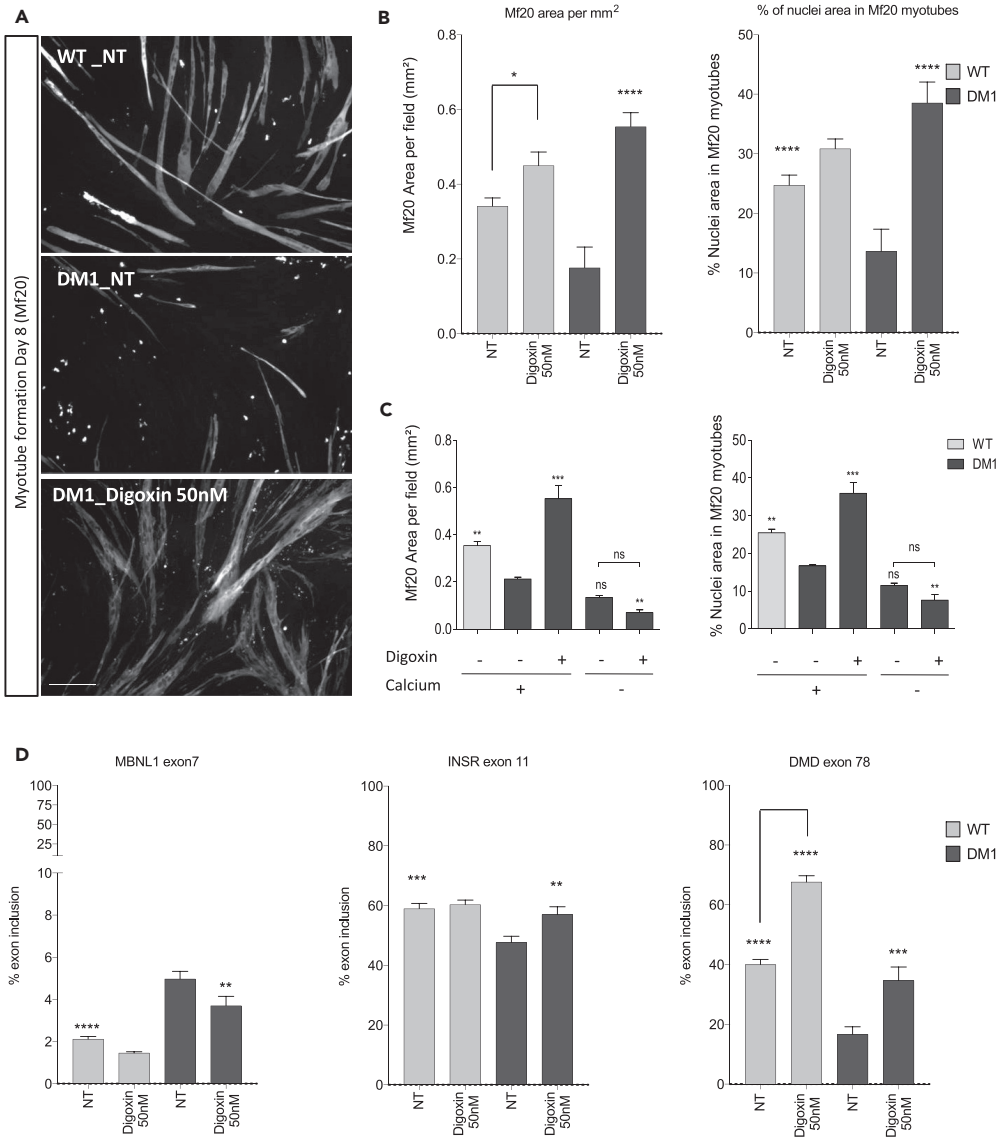

Figure 7. Digoxin Treatment Restores *In Vitro* Myogenic Defect in DM1

(A) Representative immunostaining for the myogenic marker Mf20 in WT and DM1 myoblasts differentiated for 6 days. DM1 myoblasts were treated with 50 nM of digoxin at day 1 of differentiation.

(B) Automated quantification of myogenic differentiation as determined by the measurement of the total area stained for Mf20 per field in WT-differentiated myoblasts and in DM1-differentiated myoblasts, treated or untreated with 50 nM digoxin, as well as the quantification of nucleus area per Mf20-positive myotube. All data were analyzed with one way ANOVA followed by a "Bonferroni's Multiple Comparison Test" *p<0.01, ****p<0.0001.

(C) Calcium-dependent effect of digoxin on the *in vitro* myogenic impairment observed in DM1 myoblasts. Cells were differentiated in the presence or absence of calcium. The effect of digoxin treatment (50 nM for 7 days) on myogenesis was evaluated by automated quantification according to the total area stained for Mf20 per field and as the percentage of the total area of nuclei identified within Mf20-positive myotubes. Data are presented as mean ± SD (n = 3 independent experiments, 3 replicates) and were analyzed with one-way ANOVA, followed by a "Bonferroni's multiple comparison test"; **p < 0.05, ***p < 0.001.

(D) Analysis of splice variants in WT and DM1 myoblasts differentiated for 8 days. Digoxin 50nM was applied as a chronic (7 days) or pulse (2 days) treatment. Percentage of exon inclusion was quantified by RT-PCR and Capillary Electrophoresis using the Agilent bioanalyzer 2100. Data represent mean ± SD (n=1 experiment – triplicates). All data were analyzed with one way ANOVA followed by a "Bonferroni's Multiple Comparison Test" **p<0.05, ***p<0.001.

compounds. Cardiac glycosides modulate the Na^+/K^+ ATPase protein complex upon binding and activate downstream signaling pathways via increased intracellular calcium concentrations (Fontana et al., 2013), which can independently induce changes in alternative mRNA splicing patterns (Razanau and Xie, 2013; Sharma and Lou, 2011; Sharma et al., 2014). In this case, the molecular mechanisms linking calcium concentration to the modulation of the splicing process may involve chromatin modifications, rather than RNA-binding proteins (Sharma et al., 2014). Thus the effects of metformin and cardiac glycosides do not rely on fully identical intracellular pathways. Therefore they may also modify various subsets of DM1-affected genes. It is thus tempting to speculate that a combination of several drugs may lead to additive or synergistic beneficial effects (Konieczny et al., 2017). From this perspective, it will also be interesting to analyze the effects of other drugs known to affect alternative RNA splicing, e.g., valproate, amyloride, or kinetin (Axelrod et al., 2011; Chang et al., 2011; Farrelly-Rosch et al., 2017), in the context of DM1 *in vitro* models. Calcium changes in treated cells may not, however, be the sole mechanism underlying the effects of cardiac glycosides. In the present study, use of PD0325901, an inhibitor of the ERK pathway, appeared as yet another path for regulating alternative mRNA splicing, which may normalize a further subset of DM1-affected genes. DM1 myoblasts have been described to sustain abnormal ERK activity that might be responsible for the defective myogenic differentiation (Beffy et al., 2010). It would therefore be interesting to determine whether the digoxin effect on the functional *in vitro* myogenesis was triggered by a splicing modification or through an ERK1/2 inhibitory effect. In addition, our results also demonstrated that digoxin treatment led to an increased level of the inactive form of GSK3-β (phosphorylated at S9) in DM1_MSCs. Interestingly, inhibition of GSK3-β signaling with tideglusib is actually under clinical investigation in patients with DM1 (ClinicalTrials.gov identifier: NCT02858908). This development was based on different studies demonstrating that the active GSK3-β is elevated in skeletal muscle biopsy samples from patients with DM1 and in skeletal muscle of mice. Inhibition of GSK3-β signaling in both DM1 cell culture and mouse models reduced muscle weakness and myotonia in DM1 mice (Jones et al., 2012; Wei et al., 2018). In our study, the use of CHIR99021, a well-characterized GSK3-β inhibitor, did not improve IR exon 11 inclusion and minimized the digoxin effect when co-treatment was applied. Even if a combination of a cardiac glycoside with a GSK3-β inhibitor might theoretically allow the modification of a larger variety of exons and phenotypes, a combinatorial therapeutic strategy needs to be carefully evaluated, as one strategy can abolish the effect of the other.

The present study further emphasizes the value of pluripotent stem cell lines derived from mutant-gene-carrying donors as *in vitro* cell models for monogenic pathologies and drug discovery. Access to a never-ending supply of cells expressing a physiologically and pathologically relevant human genome is a first advantage over other cell models. The physiological relevance of our cellular model was also of particular importance here, because ratios of gene transcripts are highly dependent upon cell phenotypes. It is interesting to note that a previous study has already demonstrated the ability of cardiac glycosides to modulate alternative mRNA splicing of a large number of genes (Stoilov et al., 2008). However, using HEK cells as a model, this list did not include the 15 DM1-affected genes identified in the present study using mesodermal and neural derivatives of ES cells. In addition, the use of stem cell derivatives allows a comparison of populations of cells displaying an exact same phenotype, which differ only in their genotype (e.g., DM1 versus WT).

In summary, stem cell derivatives provide a very interesting platform for *in vitro* drug discovery, but results need to be confirmed using other relevant *in vitro* and *in vivo* models, as performed here, before identifying compounds that can be moved forward toward clinical application.

Limitations of the Study

In this study, we identified the capacity of the FDA-approved cardiac glycosides to normalize several alternative mRNA splicing of genes affected by the causal mutation of DM1. Our results demonstrated that this effect is calcium dependent and can be synergic to the inhibition of the ERK signaling pathway. However, the exact molecular mechanisms by which cardiac glycosides can induce the normalization of these affected alternative splicing is still unclear. Our results suggest that the mechanisms of action of these compounds are not dependent on the two main splicing factors, known to be involved in the pathogenesis of DM1. Therefore additional experiments are needed to investigate the mechanisms by which cardiac glycosides normalize alternative splicing defects in DM1.

METHODS

All methods can be found in the accompanying Transparent Methods supplemental file.

SUPPLEMENTAL INFORMATION

Supplemental Information includes Transparent Methods, seven figure, and three tables and can be found with this article online at https://doi.org/10.1016/j.isci.2018.12.019.

ACKNOWLEDGMENT

I-Stem is part of the Biotherapies Institute for Rare Diseases (BIRD), supported by the Association Françaisecontre les Myopathies (AFM-Téléthon). This project was supported by AFM and INSERM. This project was also funded by grants from ANR (ANR-16-CE17-0018), AFM, and the Laboratoired'Excellence Revive (Investissementd'Avenir; ANR-10-LABX-73). We thank Vincent Mouly (INSERM U 787, Paris), Nicolas Charlet (IGBMC, Illkirch), and Genevieve Gourdon (INSERM U781, Paris) for helpful contributions and critical reviews of the manuscript.

AUTHOR CONTRIBUTIONS

Conceptualization, Y.M., M.L., M.P., G.P., S.B., and C.M.; Methodology, Y.M., P.P., B.B., L.L., J.G., and C.M.; Investigation, Y.M., P.P., B.B., L.L., S.R., D.F., J.C., and C.M.; Formal Analysis, Y.M., M.L.,J.D., H.P., G.P., D.A., S.B., and C.M.; Writing – Original Draft, C.M., Y.M., and M.P.; Writing – Review and Editing, Y.M., S.B., L.L., and C.M.; Funding acquisition, C.M. and M.P.

DECLARATION OF INTERESTS

The authors declare no competing interests.

Received: July 9, 2018
Revised: December 14, 2018
Accepted: December 20, 2018
Published: January 25, 2019

REFERENCES

Anderson, E.S., Lin, C.H., Xiao, X., Stoilov, P., Burge, C.B., and Black, D.L. (2012). Thecardiotonic steroid digitoxin regulates alternative splicing through depletion of the splicing factors SRSF3 and TRA2B. RNA *18*, 1041–1049.

Axelrod, F.B., Liebes, L., Gold-Von Simson, G., Mendoza, S., Mull, J., Leyne, M., Norcliffe-Kaufmann, L., Kaufmann, H., and Slaugenhaupt, S.A. (2011). Kinetin improves IKBKAP mRNA splicing in patients with familial dysautonomia. Pediatr. Res. *70*, 480–483.

Beffy, P., Del Carratore, R., Masini, M., Furling, D., Puymirat, J., Masiello, P., and Simili, M. (2010). Altered signal transduction pathways and induction of autophagy in human myotonic dystrophy type 1 myoblasts. Int. J. Biochem. Cell Biol. *42*, 1973–1983.

Bigot, A., Klein, A.F., Gasnier, E., Jacquemin, V., Ravassard, P., Butler-Browne, G., Mouly, V., and Furling, D. (2009). Large CTG repeats trigger p16-dependent premature senescence in myotonic dystrophy type 1 muscle precursor cells. Am. J. Pathol. *174*, 1435–1442.

Chang, W.H., Liu, T.C., Yang, W.K., Lee, C.C., Lin, Y.H., Chen, T.Y., and Chang, J.G. (2011). Amiloride modulates alternative splicing in leukemic cells and resensitizes Bcr-AblT315I mutant cells to imatinib. Cancer Res. *71*, 383–392.

Charbord, J., Poydenot, P., Bonnefond, C., Feyeux, M., Casagrande, F., Brinon, B., Francelle, L., Auregan, G., Guillermier, M., Cailleret, M., et al. (2013). High throughput screening for inhibitors of REST in neural derivatives of human embryonic stem cells reveals a chemical compound that promotes expression of neuronal genes. Stem Cells *31*, 1816–1828.

Childs-Disney, J.L., Parkesh, R., Nakamori, M., Thornton, C.A., and Disney, M.D. (2012). Rational design of bioactive, modularly assembled aminoglycosides targeting the RNA that causes myotonic dystrophy type 1. ACS Chem. Biol. *7*, 1984–1993.

Childs-Disney, J.L., Stepniak-Konieczna, E., Tran, T., Yildirim, I., Park, H., Chen, C.Z., Hoskins, J., Southall, N., Marugan, J.J., Patnaik, S., et al. (2013). Induction and reversal of myotonic dystrophy type 1 pre-mRNA splicing defects by small molecules. Nat. Commun. *4*, 2044.

Darville, H., Poulet, A., Rodet-Amsellem, F., Chatrousse, L., Pernelle, J., Boissart, C., Heron, D., Nava, C., Perrier, A., Jarrige, M., et al. (2016). Human pluripotent stem cell-derived cortical neurons for high throughput medication screening in autism: a proof of concept study in SHANK3 haploinsufficiency syndrome. EBioMedicine *9*, 293–305.

Dedkova, E.N., Sigova, A.A., and Zinchenko, V.P. (2000). Mechanism of action of calcium ionophores on intact cells: ionophore-resistant cells. Membr.Cell Biol. *13*, 357–368.

Denis, J.A., Gauthier, M., Rachdi, L., Aubert, S., Giraud-Triboult, K., Poydenot, P., Benchoua, A., Champon, B., Maury, Y., Baldeschi, C., et al. (2013). mTOR-dependent proliferation defect in human ES-derived neural stem cells affected by myotonic dystrophy type 1. J. Cell Sci. *126*, 1763–1772.

Du, H., Cline, M.S., Osborne, R.J., Tuttle, D.L., Clark, T.A., Donohue, J.P., Hall, M.P., Shiue, L., Swanson, M.S., Thornton, C.A., et al. (2010). Aberrant alternative splicing and extracellular matrix gene expression in mouse models of myotonic dystrophy. Nat. Struct. Mol. Biol. *17*, 187–193.

Du, J., Campau, E., Soragni, E., Jespersen, C., and Gottesfeld, J.M. (2013). Length-dependent CTG.CAG triplet-repeat expansion in myotonic dystrophy patient-derived induced pluripotent stem cells. Hum. Mol. Genet. *22*, 5276–5287.

Farrelly-Rosch, A., Lau, C.L., Patil, N., Turner, B.J., and Shabanpoor, F. (2017). Combination of valproic acid and morpholino splice-switching oligonucleotide produces improved outcomes in spinal muscular atrophy patient-derived fibroblasts. Neurochem.Int. *108*, 213–221.

Finsterer, J., and Stollberger, C. (2012). Beneficial effect of digitoxin for heart failure from noncompaction in myotonic dystrophy 1. Int. J. Cardiol. *160*, e50–e51.

Fontana, J.M., Burlaka, I., Khodus, G., Brismar, H., and Aperia, A. (2013). Calcium oscillations triggered by cardiotonic steroids. FEBS J. *280*, 5450–5455.

Francois, V., Klein, A.F., Beley, C., Jollet, A., Lemercier, C., Garcia, L., and Furling, D. (2011). Selective silencing of mutated mRNAs in DM1 by using modified hU7-snRNAs. Nat. Struct. Mol. Biol. *18*, 85–87.

Gauthier, M., Marteyn, A., Denis, J.A., Cailleret, M., Giraud-Triboult, K., Aubert, S., Lecuyer, C., Marie, J., Furling, D., Vernet, R., et al. (2013). A defective Krab-domain zinc-finger transcription factor contributes to altered myogenesis in myotonic dystrophy type 1. Hum. Mol. Genet. *22*, 5188–5198.

Hothi, S.S., Chinnappa, S., and Tan, L.B. (2014). 200+ years of a misunderstood drug for treating chronic heart failure: digoxin, why and how should we continue using it? Int. J. Cardiol. *168*, 645–647.

Jones, K., Wei, C., Iakova, P., Bugiardini, E., Schneider-Gold, C., Meola, G., Woodgett, J., Killian, J., Timchenko, N.A., and Timchenko, L.T. (2012). GSK3beta mediates muscle pathology in myotonic dystrophy. J. Clin. Invest. *122*, 4461–4472.

Kanadia, R.N., Johnstone, K.A., Mankodi, A., Lungu, C., Thornton, C.A., Esson, D., Timmers, A.M., Hauswirth, W.W., and Swanson, M.S. (2003). A muscleblind knockout model for myotonic dystrophy. Science *302*, 1978–1980.

Kanji, S., and MacLean, R.D. (2012). Cardiac glycoside toxicity: more than 200 years and counting. Crit. Care Clin. *28*, 527–535.

Ketley, A., Chen, C.Z., Li, X., Arya, S., Robinson, T.E., Granados-Riveron, J., Udosen, I., Morris, G.E., Holt, I., Furling, D., et al. (2013). High-content screening identifies small molecules that remove nuclear foci, affect MBNL distribution and CELF1 protein levels via a PKC-independent pathway in myotonic dystrophy cell lines. Hum. Mol. Genet. *23*, 1551–1562.

Konieczny, P., Selma-Soriano, E., Rapisarda, A.S., Fernandez-Costa, J.M., Perez-Alonso, M., and Artero, R. (2017). Myotonicdystrophy: candidate small molecule therapeutics. Drug Discov. Today *22*, 1740–1748.

Lagoeiro Jorge, B., Lanzieri, P., Braida do Carmo, F., Haffner, P.M., Lagoeiro Jorge, A., and Wolney de Andrade, M. (2012). Cardiomyopathy secondary to Steinert's dystrophy. Insuficiencia Cardiaca *7*, 143–147.

Laustriat, D., Gide, J., Barrault, L., Chautard, E., Benoit, C., Auboeuf, D., Boland, A., Battail, C., Artiguenave, F., Deleuze, J.F., et al. (2015). In vitro and in vivo modulation of alternative splicing by the biguanide metformin. Mol. Ther. Nucleic Acids *4*, e262.

Lee, G., Ramirez, C.N., Kim, H., Zeltner, N., Liu, B., Radu, C., Bhinder, B., Kim, Y.J., Choi, I.Y., Mukherjee-Clavin, B., et al. (2012a). Large-scale screening using familial dysautonomia induced pluripotent stem cells identifies compounds that rescue IKBKAP expression. Nat. Biotechnol. *30*, 1244–1248.

Lee, J.E., Bennett, C.F., and Cooper, T.A. (2012b). RNase H-mediated degradation of toxic RNA in myotonic dystrophy type 1. Proc. Natl. Acad. Sci. U S A *109*, 4221–4226.

Logigian, E.L., Martens, W.B., Moxley, R.T.t., McDermott, M.P., Dilek, N., Wiegner, A.W., Pearson, A.T., Barbieri, C.A., Annis, C.L., Thornton, C.A., et al. (2010). Mexiletine is an effective antimyotonia treatment in myotonic dystrophy type 1. Neurology *74*, 1441–1448.

Mahadevan, M., Tsilfidis, C., Sabourin, L., Shutler, G., Amemiya, C., Jansen, G., Neville, C., Narang, M., Barcelo, J., O'Hoy, K., et al. (1992). Myotonic dystrophy mutation: an unstable CTG repeat in the 3' untranslated region of the gene. Science *255*, 1253–1255.

Mankodi, A., Takahashi, M.P., Jiang, H., Beck, C.L., Bowers, W.J., Moxley, R.T., Cannon, S.C., and Thornton, C.A. (2002). Expanded CUG repeats trigger aberrant splicing of ClC-1 chloride channel pre-mRNA and hyperexcitability of skeletal muscle in myotonic dystrophy. Mol. Cell *10*, 35–44.

Mankodi, A., Urbinati, C.R., Yuan, Q.P., Moxley, R.T., Sansone, V., Krym, M., Henderson, D., Schalling, M., Swanson, M.S., and Thornton, C.A. (2001). Muscleblind localizes to nuclear foci of aberrant RNA in myotonic dystrophy types 1 and 2. Hum. Mol. Genet. *10*, 2165–2170.

Marteyn, A., Maury, Y., Gauthier, M.M., Lecuyer, C., Vernet, R., Denis, J.A., Pietu, G., Peschanski, M., and Martinat, C. (2011). Mutant human embryonic stem cells reveal neurite and synapse formation defects in type 1 myotonic dystrophy. Cell Stem Cell *8*, 434–444.

Mulders, S.A., van den Broek, W.J., Wheeler, T.M., Croes, H.J., van Kuik-Romeijn, P., de Kimpe, S.J., Furling, D., Platenburg, G.J., Gourdon, G., Thornton, C.A., et al. (2009). Triplet-repeat oligonucleotide-mediated reversal of RNA toxicity in myotonic dystrophy. Proc. Natl. Acad. Sci. U S A *106*, 13915–13920.

Nakamori, M., Sobczak, K., Puwanant, A., Welle, S., Eichinger, K., Pandya, S., Dekdebrun, J., Heatwole, C.R., McDermott, M.P., Chen, T., et al. (2013). Splicing biomarkers of disease severity in myotonic dystrophy. Ann. Neurol. *74*, 862–872.

Nakamori, M., Taylor, K., Mochizuki, H., Sobczak, K., and Takahashi, M.P. (2016). Oral administration of erythromycin decreases RNA toxicity in myotonic dystrophy. Ann. Clin. Transl. Neurol. *3*, 42–54.

Pandey, S.K., Wheeler, T.M., Justice, S.L., Kim, A., Younis, H.S., Gattis, D., Jauvin, D., Puymirat, J., Swayze, E.E., Freier, S.M., et al. (2015). Identification and characterization of modified antisense oligonucleotides targeting DMPK in mice and nonhuman primates for the treatment of myotonic dystrophy type 1. J. Pharmacol. Exp. Ther. *355*, 329–340.

Parkesh, R., Childs-Disney, J.L., Nakamori, M., Kumar, A., Wang, E., Wang, T., Hoskins, J., Tran, T., Housman, D., Thornton, C.A., et al. (2012). Design of a bioactive small molecule that targets the myotonic dystrophy type 1 RNA via an RNA motif-ligand database and chemical similarity searching. J. Am. Chem. Soc. *134*, 4731–4742.

Phillips, M.F., and Harper, P.S. (1997). Cardiac disease in myotonic dystrophy. Cardiovasc. Res. *33*, 13–22.

Razanau, A., and Xie, J. (2013). Emerging mechanisms and consequences of calcium regulation of alternative splicing in neurons and endocrine cells. Cell.Mol. Life Sci. *70*, 4527–4536.

Savkur, R.S., Philips, A.V., and Cooper, T.A. (2001). Aberrant regulation of insulin receptor alternative splicing is associated with insulin resistance in myotonic dystrophy. Nat. Genet. *29*, 40–47.

Schmitt, J., and Schmidt, C. (1975). [Steinert's syndrome and the myocardium. Total gene expression by the myocardium]. J. Genet. Hum. *23*, 59–64.

Schoner, W., and Scheiner-Bobis, G. (2007). Endogenous and exogenous cardiac glycosides and their mechanisms of action. Am. J. Cardiovasc. Drugs *7*, 173–189.

Sharma, A., and Lou, H. (2011). Depolarization-mediated regulation of alternative splicing. Front. Neurosci. *5*, 141.

Sharma, A., Nguyen, H., Geng, C., Hinman, M., Luo, G., and Lou, H. (2014). Calcium-mediated histone modifications regulate alternative splicing in cardyomyocytes. Proc. Natl. Acad. Sci. U S A *111*, E4920–E4928.

Stoilov, P., Lin, C.H., Damoiseaux, R., Nikolic, J., and Black, D.L. (2008). A high-throughput screening strategy identifies cardiotonic steroids as alternative splicing modulators. Proc. Natl. Acad. Sci. U S A *105*, 11218–11223.

Thornell, L.E., Lindstom, M., Renault, V., Klein, A., Mouly, V., Ansved, T., Butler-Browne, G., and Furling, D. (2009). Satellite cell dysfunction contributes to the progressive muscle atrophy in myotonic dystrophy type 1. Neuropathol. Appl. Neurobiol. *35*, 603–613.

Thornton, C.A., Wang, E., and Carrell, E.M. (2017). Myotonic dystrophy: approach to therapy. Curr.Opin.Genet. Dev. *44*, 135–140.

Turner, C., and Hilton-Jones, D. (2014). Myotonic dystrophy: diagnosis, management and new therapies. Curr.Opin. Neurol. *27*, 599–606.

Ueki, J., Nakamori, M., Nakamura, M., Nishikawa, M., Yoshida, Y., Tanaka, A., Morizane, A., Kamon, M., Araki, T., Takahashi, M.P., et al. (2017). Myotonic dystrophy type 1 patient-derived iPSCs for the investigation of CTG repeat instability. Sci. Rep. *7*, 42522.

Wei, C., Stock, L., Valanejad, L., Zalewski, Z.A., Karns, R., Puymirat, J., Nelson, D., Witte, D., Woodgett, J., Timchenko, N.A., et al. (2018). Correction of GSK3beta at young age prevents muscle pathology in mice with myotonic dystrophy type 1. FASEB J. *32*, 2073–2085.

Wheeler, T.M., Leger, A.J., Pandey, S.K., MacLeod, A.R., Nakamori, M., Cheng, S.H., Wentworth, B.M., Bennett, C.F., and Thornton, C.A. (2012). Targeting nuclear RNA for in vivo correction of myotonic dystrophy. Nature *488*, 111–115.

Wheeler, T.M., Lueck, J.D., Swanson, M.S., Dirksen, R.T., and Thornton, C.A. (2007). Correction of ClC-1 splicing eliminates chloride channelopathy and myotonia in mouse models of myotonic dystrophy. J. Clin. Invest. *117*, 3952–3957.

ISCI, Volume *11*

Supplemental Information

Pluripotent Stem Cell-Based Drug Screening Reveals Cardiac Glycosides as Modulators of Myotonic Dystrophy Type 1

Yves Maury, Pauline Poydenot, Benjamin Brinon, Lea Lesueur, Jacqueline Gide, Sylvain Roquevière, Julien Côme, Hélène Polvèche, Didier Auboeuf, Jérome Alexandre Denis, Geneviève Pietu, Denis Furling, Marc Lechuga, Sandrine Baghdoyan, Marc Peschanski, and Cécile Martinat

Transparent methods

Cell culture

Human embryonic stem cells (hESCs) were maintained and differentiated into Mesenchymal Stem Cells as previously described (Marteyn et al., 2011). Briefly, hES were manually dissociated and plated on 0.1% gelatin-coated dishes (Sigma) in Knockout DMEM medium optimized for ES cells (Invitrogen), supplemented with 20% of Fetal Bovine Serum (FBS, Eurobio), 1mM L-glutamine (Invitrogen), 1% non-essential amino-acid (Invitrogen), and 0,1% β-mercaptoethanol (Invitrogen). Medium was changed every over two days. Confluent cells were passed with trypsin/EDTA 1X (Invitrogen) in new gelatin-coated plates and plated at a density of 8.000/cm2. After three weeks of differentiation, MSC phenotype was assessed by FACS analysis for CD44, Stro1, CD73 and endoglin expression (all from ABCAM, 1/100). MSC cells amplification was performed as previously described (Marteyn et al., 2011). Repeats size was estimated at 1.300 (Marteyn et al., 2011).

Control and DM1 patient myoblasts (2000 CTG repeats) provided by Denis Furling, were cultured in DMEM/F-12 medium (Invitrogen) supplemented with 20% FBS (Eurobio) and 0.1% of penicillin–streptomycin (Invitrogen). For differentiation, medium was changed to 2% FBS in 75% Alpha MEM (Invitrogen) and 25% M199 medium (Invitrogen), supplemented with 1% penicillin–streptomycin and 10µg/mL insulin (Sigma). Medium was changed every 2 or 3 days.

Chemicals

Three different libraries were screened including 1.280 small molecules from the Prestwick library, 9.689 from ChemXinfinity and 1.280 from Lopac libray (Sigma-Aldrich). Individual small molecules, Digitoxigenin, Ouabain, Strophanditin, Digoxigenin, Oleandin, Cymarin, Digoxin, Cycloheximide, A23187, were purchased from Sigma-Aldrich, PD0325901 from Euromedex, LY294002 from OZYME, CHIR99021 from Tocris.

Primary Screening

hESCs derived MSC were plated at 3.000 cells per well in 384-well plates (Corning) coated with 0.1% gelatin. Cell seeding was performed using the automate Biocell 1800 (Agilent). Each compound was

tested at a final concentration of 10µM in 0.1% DMSO. Cells were treated with each compound in duplicate for 48h. Sequential dilution of compounds and cell treatment was performed using the automate BioCell 1800 (Agilent). Secondary validation tests were performed over a 10-point dilution range in 96 or 384 well plate format. For experiments in calcium free conditions, prior to compound addition, medium was changed to calcium free medium DMEM (Invitrogen) supplemented with 20% of Fetal Bovine Serum, 1mM L-glutamine, 1% non-essential amino-acid, 0,1% β-mercaptoethanol and 400µM EDTA (Sigma-Aldrich).

Fluorescent In situ Hybridization (FISH)

All steps were performed using the plate washer CW-ELX405 (BioTek Instruments) combined with a multidrop 384 (Thermofisher - Labsystem). Cells were fixed with PBS buffer containing 4% PFA (Electron Microscopy Science,) for 20 minutes at room temperature and washed with 200µL of PBS. Cells were then incubated overnight at 4 °C with 70% Ethanol. After PBS wash, cells were rehydrated with a solution of PBS containing 5mM MgCl2 for 15-30 min and then sequentially incubated with prehybridization buffer (50mM Phosphate buffer, 40% formamide, 2X SSC, 50µl/ well) for 15-30 min and hybridization buffer (Prehybrydization buffer with 0,2% BSA and 7% Dextran, 50µl/well) containing 300ng/mL of the (CAG)10-Cy5 probe (5'Alexa 647-TTCTTATTCTTCAgCAgCAgCAgCAgCAgCAgCAgCAg3') (Operon) overnight at 37°C. Washing steps consisted in pre-warmed Washing buffer (Prehybrydization buffer + 0.2% BSA, 60µL/well) for 15 min at RT followed by addition of washing buffer (80µL) and incubation for 30 min at 37°C. Cells were then washed twice in PBS before nuclei counterstaining Hoechst 33258 (Invitrogen, 5µg/mL). Plates were stored at 4°C until analysis.

Immunostaining

After fixation with PFA4% for 10', Cells were incubated over night at 4°C with the following list of primary antibodies : Mf20 (DSHB, 1/200), desmin (R&D system, 1/25), MBNL1 (Santa cruz, 1/1000), Mb1a(4A8) (Provided by Dr. Glenn Morris). Appropriated Alexa fluorescent secondary antibodies (1/1000, Invitrogen) and Hoechst (5µg/mL) were added for 1h30.

Image acquisition and analysis

Nuclear foci detection was performed using the Cellomics Array Scan VTI high content imaging system (Thermofisher Scientist) with the 20X objective to automatically focus cell preparation. Images were acquired in High Resolution camera mode on two channels: nuclei (channel 1, HOECHST XF93) and DMPK foci (channel 2, Cy5 Sensitive XF110). Based on the Hoechst channels, a minimum of 250 nuclei were identified using intensity thresholding, background correction and segmentation parameters. Each nuclear region was then reported on the second channel (Cy5) to limit the foci detection to the nuclear area. Foci were identified using a fixed intensity threshold, background correction and segmentation parameters. To avoid unspecific signal quantification, foci detection was gated with minimum and maximum area (0.1 μm^2 to 40μm^2) or intensity (average intensity min 70, max 1300).

The effect of digoxin treatment on myogenic differentiation was automatically processed as previously described (Polesskaya et al., 2013). Using 5X magnification, Hoechst staining was used for autofocus and nuclei were identified applying intensity threshold, segmentation and background correction parameters. In the same way, Mf20 were detected. The percent of the total detected nuclear area within MF20 myotubes was used as the percent of positive cells and the total Mf20 area per field was calculated.

Splicing analysis by RT-PCR

Total RNA was extracted using the RNeasy Micro/Mini kit (Qiagen) and reverse transcribed using random hexamers and Superscript III Reverse Transcriptase kit (Invitrogen) according to the manufacter's protocol. For splicing analysis, PCR amplification of endogenous or exogenous genes was carried out with recombinant Taq DNA polymerase (Invitrogen) and the primers listed in Table S1. The amplification was performed using a first step at 94°C for 3 min followed by 35 cycles of 45 s at 94 °C, 30 s at 55 °C, 30 s at 72 °C, and with a final 10 min extension at 72 °C. The PCR products were analyzed using DNA 1000 LabChip kit (Agilent) and quantified with the Bioanalyzer 2100.

Gene expression analysis by quantitative PCR

Quantitative PCR reactions were carried out using a Chromo4 Real-Time System (Bio-Rad) with Syber Green PCR Master Mix (Applied Biosystems). Detailed information on the primers sequences is provided in TableS1. The 2−ΔΔCt method was used to determine the relative expression level of each gene. Relative titration of *INSR* transcripts +/- exon 11, *NMDAR1* transcripts +/- exon 5 and house keeping gene 18S was monitored with TaqMan gene expression assays using the primers and MGB probes described in TableS1 and TaqMan Gene Expression Master Mix (Applied Biosystem). This was carried out using the Lightcycler 480 (Roche, France).

Protein extraction and western blot analyses

Western blots analyses were carried out as previously described(Denis et al., 2013; Gauthier et al., 2013). Briefly, cells were lyzed in RIPA 1X buffer (Sigma) containing protease inhibitors (Sigma) and phosphatases inhibitors (Roche). Nuclear and cytoplasmic fractions were obtained using the NE-PER Nuclear and Cytoplasmic Extraction Kit (Thermo Scientific) according to manufacturer's protocol. Proteins were quantified by Pierce BCA Protein Assay kit (Pierce). Protein extracts (10 to 20µg) were loaded on a 4–12% SDS-PAGE gradient (Nupage® Bis–Tris gels, Invitrogen) and transferred onto Gel Transfer Stacks Nitrocellulose membranes (Invitrogen) using the iBlot Gel Transfer System (Invitrogen). Membranes were then incubated overnight at 4°C with primary antibodies listed in Supplementary Table 3. After hybridization of the peroxidase-conjugated secondary antibody, immunoreactive bands were revealed by using Amersham ECL Plus™ Western Blotting Detection Reagents (GE Healthcare). Equal protein loading was verified by the detection of Actin.

RNA sequencing library preparation and sequencing. Sequencing libraries were prepared according to the Illumina TruSeq Stranded mRNA Sample Prep Kit (according to manufacturer's protocol) (Illumina, San Diego, CA). A 2 × 101 bp pairedend sequencing was performed on the HiSeq2000 instrument, using half a lane per sample, to produce on average 80 million read pairs per sample (160 million sequences) with an average insert length of 130 bp. Trimmomatic,52 Tophat2,53 Picard suite (http://www.broadinstittute.github.io/picard), RNA-SeQC,54 and in-house metrics were used to evaluate data quality.

RNA sequencing data analysis and identification of differential splicing events. Reads were aligned using TopHat2 (v2.0.853). TopHat2 was run with the assistance of gene annotations (Illumina's iGenomes based on EnsEMBL r70), which means that the alignment was performed in three steps: transcriptome mapping, genome mapping, and spliced mapping. The minimum and maximum intron lengths were also reevaluated, respectively, to 30 and 1,200,000 to maximize the number of introns detected. The mate inner distances were set to their corresponding values. Alignment files in bam format were then filtered to removed poor mapping quality score (<10) and not primary alignments and read pairs with one single read mapped were filtered using samtools (v0.1.855).

For the alternative splicing analysis, reads crossing the exon–exon junction ("junction reads") were extracted from the read alignment files to detect the exon skipping events. In order to avoid spurious read alignments, we applied additional filters for the junction reads considered: no indels at the junction site, no hard clipping, and a minimal overlap of 4 bp over the junction site. FasterDB gene and exon annotations were used as a guide to detect known and new exon skipping events(Laustriat et al., 2015). For each exon skipping event detected across all samples, junction reads corresponding to the inclusion of the exon and junction reads corresponding to the exclusion of the exon were quantified. The differential analysis was performed using KissDE, an R package developed as part of the KisSplice post-processing workflow (Sacomoto et al., 2012). KissDE works on pairs of variants for which read counts are available in each replicate of each condition and tests if a variant is enriched in one condition. Counts are modeled using a negative binomial distribution. KissDE fits a generalized linear model and tests for the effect of an interaction between the variant and the condition using a likelihood ratio test with a 5% false discovery rate to control for multiple testing. A percent splicing index (PSI or Ψ) value was then estimated for each sample as the ratio of inclusion junction reads to the sum of inclusion and exclusion junction reads. As the datasets are paired, the difference of Ψ values for each event (deltaPSI or ΔΨ) was calculated as the median of ΔΨ values for each replicate. A filter was then applied on exon skipping events detected to select significant variants with an adjusted P

value ≤0.05 and ΔΨ value ≥10%. The RNA seq data are available in the Gene Expression Omnibus (GEO) database (http://www.ncbi.nlm.nih.gov/geo) under the accession number GSE99944.

Treatment in mice

All the mouse procedures were done according to protocol approved by the Committee on Animal Resources at the Centre d'Experimentation Fonctionnelle of Pitie-Salpetriere animal facility and under appropriate biological containment. 2-3 months old homozygous *HSA* ^{LR} transgenic mice (strain 20b that have been described previously (Mankodi et al., 2000) were treated with phosphate-buffered saline (PBS) or digoxin at the indicated dose and period by daily intraperitoneal injection. After the treatments, mice were sacrificed, and the rectus femoris (quadriceps) muscle was obtained for splicing analysis.

Statistical analysis

Screening data were analyzed using SpotFire software (Discngine). Data were processed using Graph pad PRISM. Student's t-test (ANOVA) was used to analyze two groups of data. For comparisons of more than two groups, 'Bonferroni's multiple comparison test' (one-way ANOVA) was used.

Denis, J.A., Gauthier, M., Rachdi, L., Aubert, S., Giraud-Triboult, K., Poydenot, P., Benchoua, A., Champon, B., Maury, Y., Baldeschi, C.*, et al.* (2013). mTOR-dependent proliferation defect in human ES-derived neural stem cells affected by myotonic dystrophy type 1. J Cell Sci *126*, 1763-1772.
Gauthier, M., Marteyn, A., Denis, J.A., Cailleret, M., Giraud-Triboult, K., Aubert, S., Lecuyer, C., Marie, J., Furling, D., Vernet, R.*, et al.* (2013). A defective Krab-domain zinc-finger transcription factor contributes to altered myogenesis in myotonic dystrophy type 1. Hum Mol Genet *22*, 5188-5198.
Laustriat, D., Gide, J., Barrault, L., Chautard, E., Benoit, C., Auboeuf, D., Boland, A., Battail, C., Artiguenave, F., Deleuze, J.F.*, et al.* (2015). In Vitro and In Vivo Modulation of Alternative Splicing by the Biguanide Metformin. Molecular therapy Nucleic acids *4*, e262.
Mankodi, A., Logigian, E., Callahan, L., McClain, C., White, R., Henderson, D., Krym, M., and Thornton, C.A. (2000). Myotonic dystrophy in transgenic mice expressing an expanded CUG repeat. Science *289*, 1769-1773.
Marteyn, A., Maury, Y., Gauthier, M.M., Lecuyer, C., Vernet, R., Denis, J.A., Pietu, G., Peschanski, M., and Martinat, C. (2011). Mutant human embryonic stem cells reveal neurite and synapse formation defects in type 1 myotonic dystrophy. Cell Stem Cell *8*, 434-444.
Polesskaya, A., Degerny, C., Pinna, G., Maury, Y., Kratassiouk, G., Mouly, V., Morozova, N., Kropp, J., Frandsen, N., and Harel-Bellan, A. (2013). Genome-wide exploration of miRNA function in mammalian muscle cell differentiation. PLoS One *8*, e71927.

Sacomoto, G.A., Kielbassa, J., Chikhi, R., Uricaru, R., Antoniou, P., Sagot, M.F., Peterlongo, P., and Lacroix, V. (2012). KISSPLICE: de-novo calling alternative splicing events from RNA-seq data. BMC bioinformatics *13 Suppl 6*, S5.

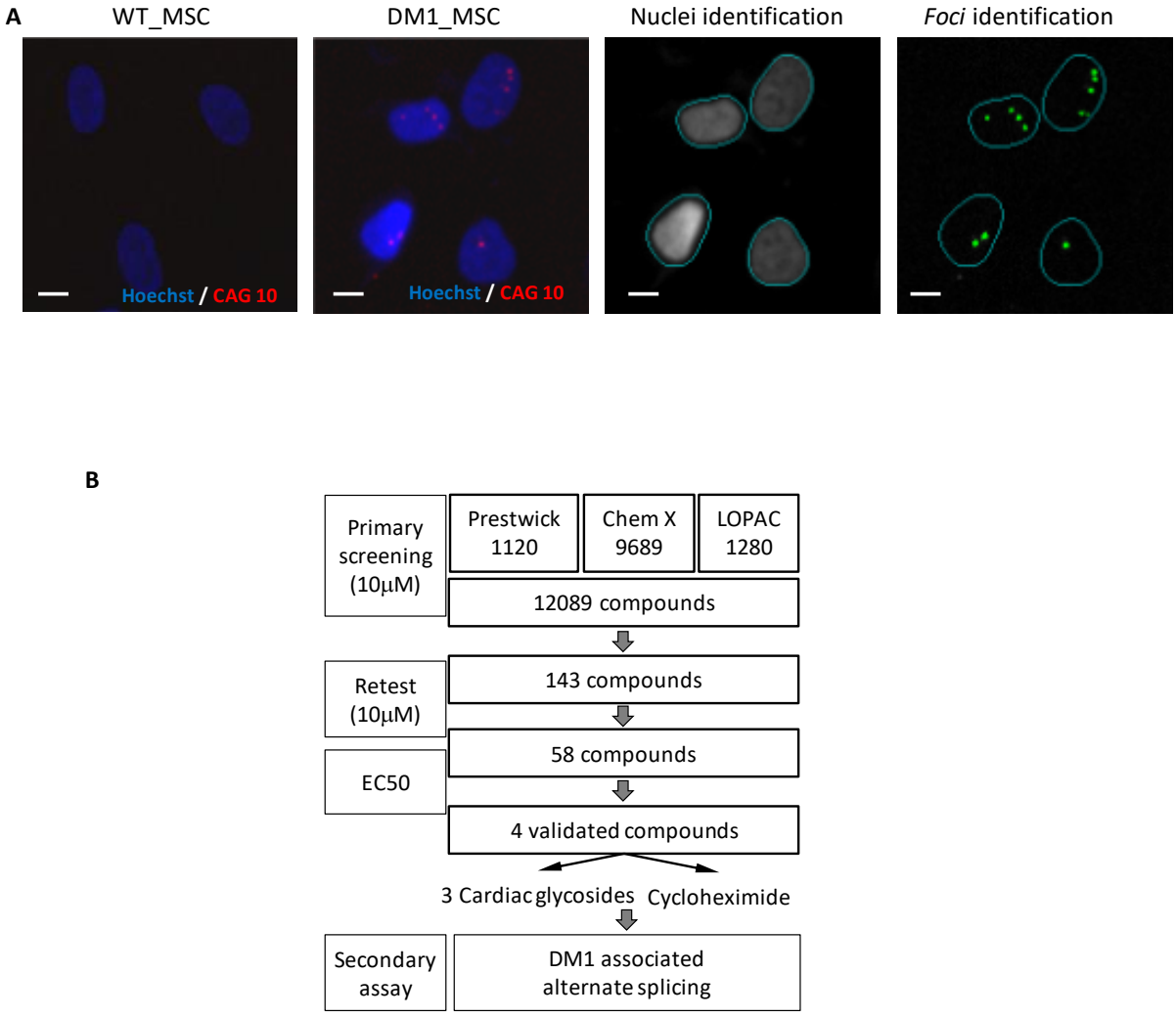

Figure S1: Global workflow for hit selection, Related to Figure 1

A- Representative images of WT and DM1 hESC derived MSC (WT_MSC and DM1_MSC) after Hoechst staining and Fluorescent in situ hybridization for DMPK mRNA (WT_MSC) (Scale bare = 10µm).

B- Schematic representation of the cascade of experiments performed in this study.

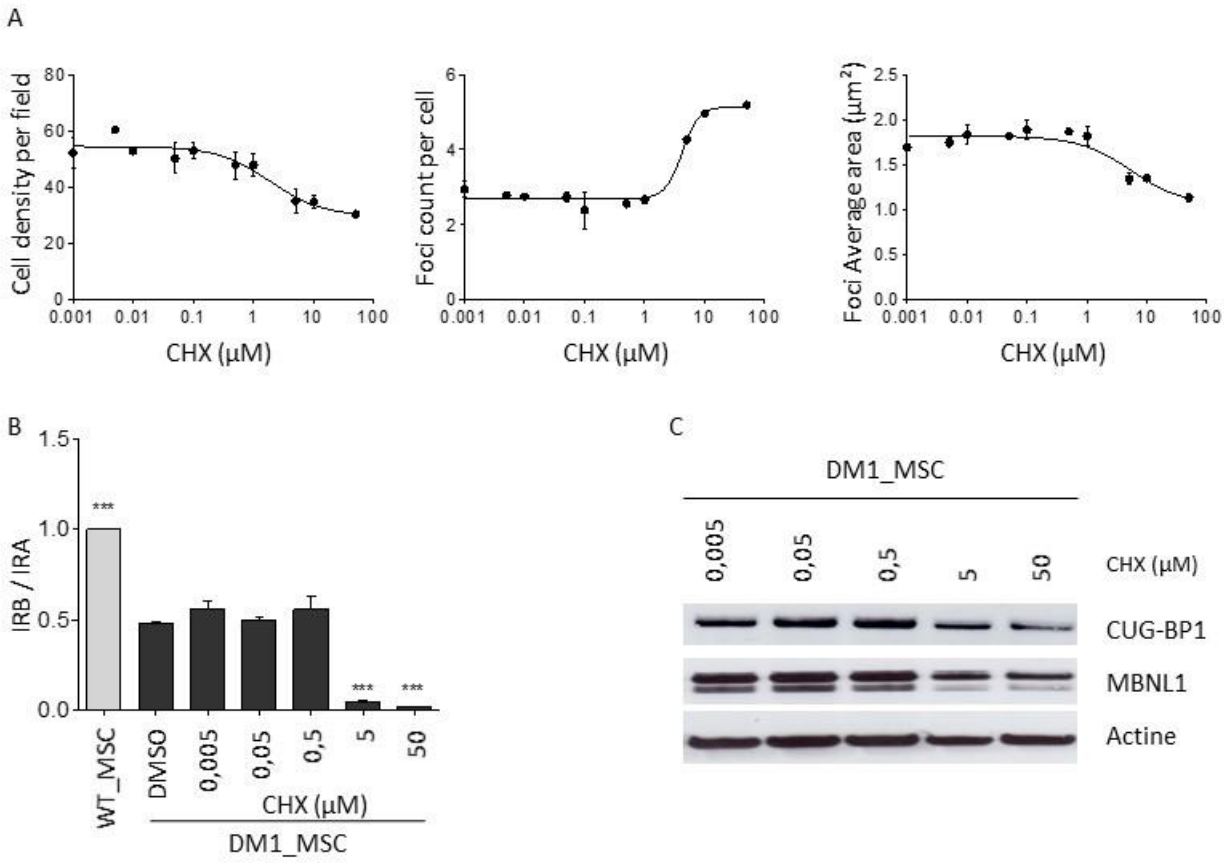

Figure S2: Cycloheximide exacerbates DM1 associated phenotypes, Related to Figure 1

A- Dose response curves for effect of cycloheximide (CHX) on cell density, number and area of mutant DMPK mRNA foci determined on DM1_MSC treated for 48h. Data represent mean ± SEM (n=2, 1 experiment). **B-** Quantification of IR alternate splicing in DM1_MSC treated with different concentrations of CHX for 48h. Relative expression level of the two isoforms of IR (IRA (-exon 11) and IRB (+ exon 11)) were measured by quantitative real time RT-PCR. WT_MSC was used as a positive control. Data represented the ratio of IRB/IRA and are indicated as mean ± SD (n=2 experiments-3 replicates) and were analyzed with one way ANOVA followed by a Bonferroni post hoc test versus DMSO treated cells. *: p-value < 0.05. **: p-value < 0.01. ***: p-value < 0.001. **C-** Western blot analysis for expression of MBNL1 and CUGBP1 after treatment of DM1_MSC treated with different concentrations of CHX for 48h. β-actin expression was used as an internal control of loading. **D-** Dose response analysis for cell density determined by number of nuclei per field on DM1_MSC after 48h treatment with seven cardiac glycosides. Data represent mean ± SEM (n=2).

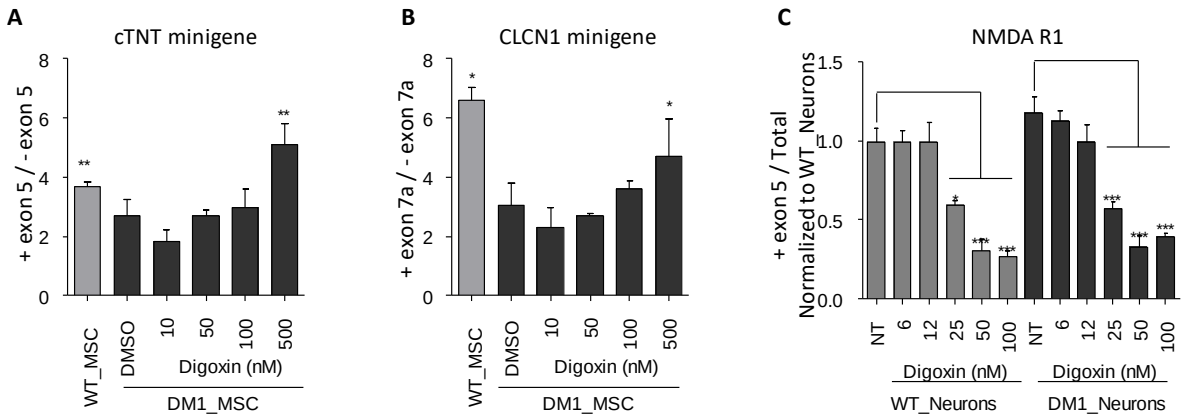

Figure S3: Beneficial effect of digoxin treatment on other splice defects associated to DM1, Related to Figure 3

A-D. Dose-response analysis of digoxin treatment on alternate splicing of exon 5 of cTNT, exon 7a of CLCN1 and exon 5 of NMDAR1. For cTNT and CLCN1, DM1_hESC MSC were transfected with a minigene containing the exon of interest (n=3, 1 experiment). Alternate splicing of NMDAR1 as analyzed on WT and DM1 hESC-derived neurons (n= 3, 1 experiment). Data represent mean ± SD and analyzed with one way ANOVA followed by a Bonferroni post hoc test. *: p-value < 0.05. **: p-value < 0.01. ***: p-value < 0.001.

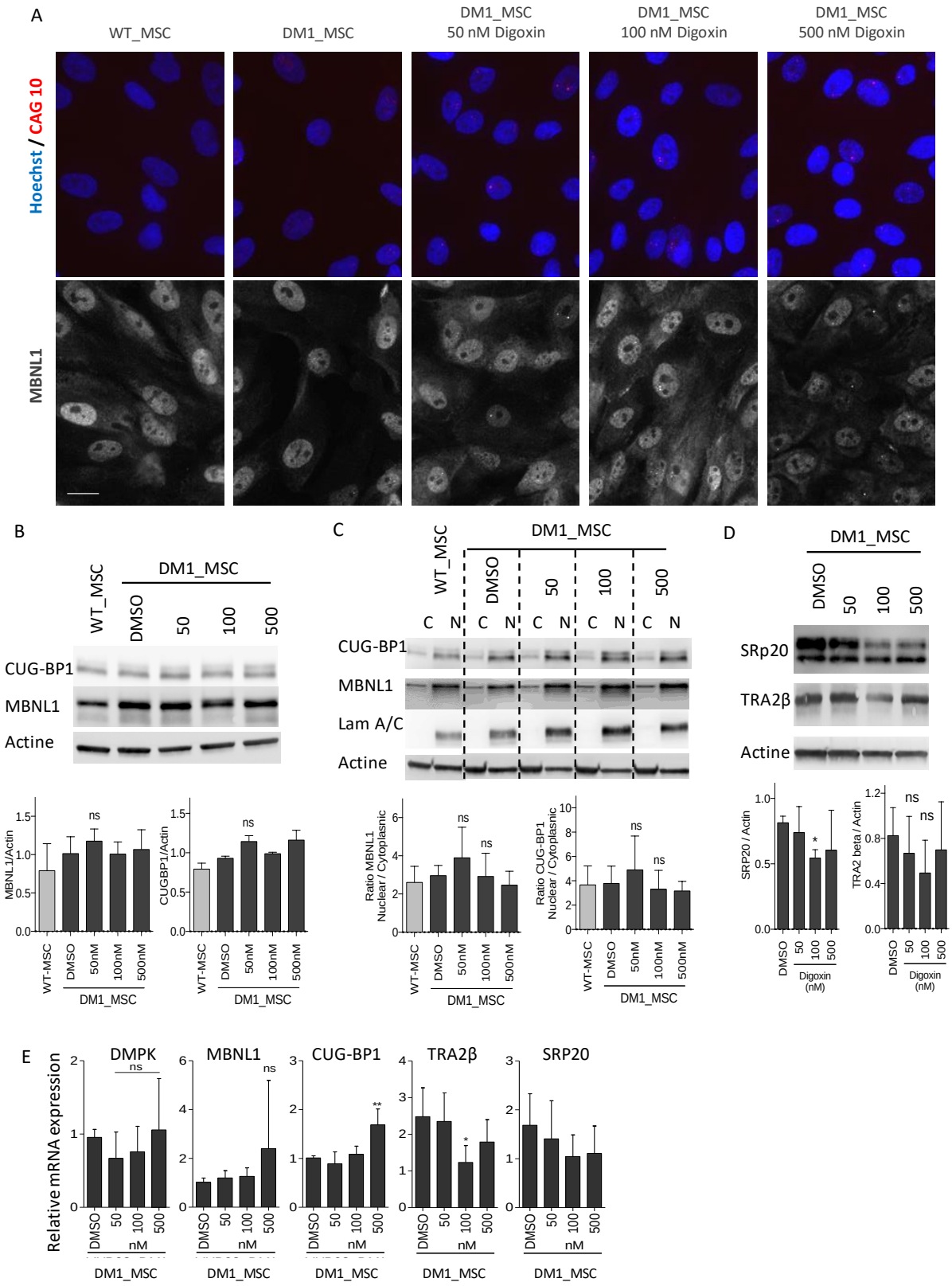

Figure S4: Digoxin-mediated effect on DM1 alternate splicing is independent of MBNL1 and CUGBP1, Related to Figure 3 and Figure 6

A- Representative images of the co-localization of MBNL1 within mutant DMPK foci by FISH combined with immunostaining for MBNL1 in DM1_MSC treated with different concentrations of digoxin for 48h (Scale bar=10μm). **B-** Western blot analysis of MBNL1 and CUGBP1 expression in DM1_MSC treated with different concentrations of digoxin for 48h. WT_MSC were used as a control (n=2). Quantification was performed by using ImageJ software. Data are presented as mean ± S.D and p-value were determined using paired t-test . *: p-value < 0.05. **: p-value < 0.01. ***: p-value < 0.001. **C-** Western blot analysis of the nuclear (N) and cytoplasmic (C) fractions of MBNL1 and CUG-BP1 in DM1_MSC treated with different concentrations of digoxin for 48h. LaminA/C was used as a nuclear positive fraction control; β-actin was used as a loading control (n=5 independent experiments). Quantification and data presentation were performed as previously described. **D-** Western blot analysis of SRp20 and TRA2β expression after treatment of DM1 hESC-MSC with different concentrations of digoxin. Cells were treated for 48h. β-actin was used as a loading control (n=2 independent experiments). Quantification and data representation were performed as previously described. **E-** Quantitative real-time RT-PCR to measure the expression level of DMPK, MBNL1, CUG-BP1, TRA2β and SRp20 after treatment of DM1_MSC treated with different concentrations of digoxin for 48h. Results were normalized with the average of control samples. Data represent mean± SD (n= 3, 3 independent experiments) and were analyzed with one way ANOVA followed by a Bonferroni post hoc test versus DMSO treated cells. *: p-value < 0.05. **: p-value < 0.01. ***: p-value < 0.001.

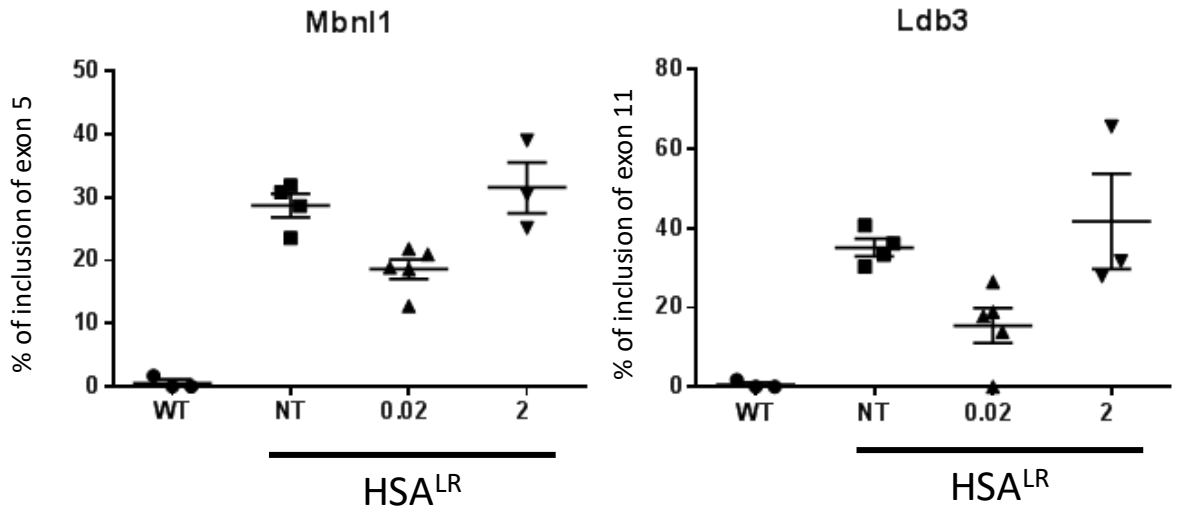

Figure S5: Intraperitoneal injection of low dose of digoxin improves splicing defects in Mbnl1 and Ldb3 in a DM1 mouse model, related to Figure 5. Analysis of Mbnl1 (left) and Ldb3 (right) alternative splicing by RT-PCR in gastrocnemius muscles of mice treated with intraperitoneal injection of two doses of digoxin (0.02 mg/kg and 2 mg/kg) for 7 days.

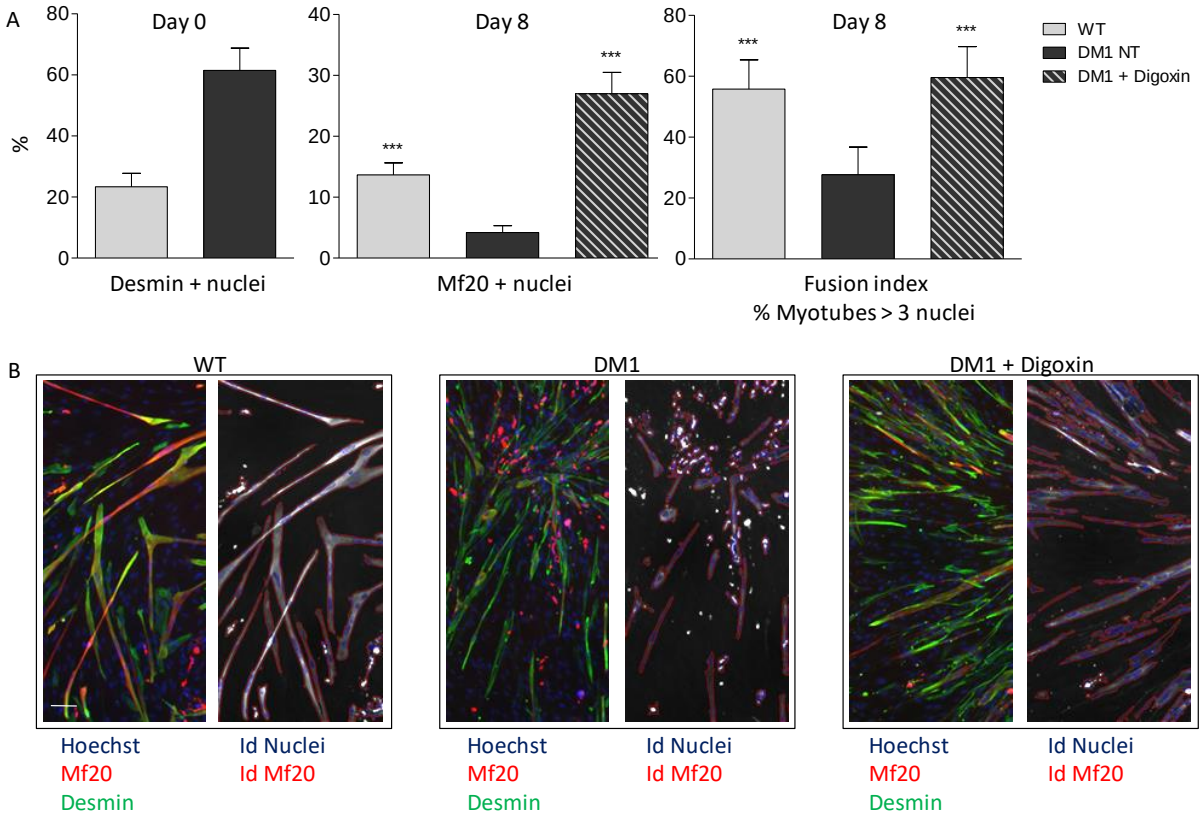

Figure S6: Functional effect of digoxin treatment on *in vitro* myogenic differentiation of DM1 myoblasts, Related to Figure 7.

A- Manual quantification of the number of Desmin positive nuclei in WT and DM1 myoblasts at day 0. Data are indicated as a percentage and represent mean± SD (n=3). **B-C** Manual quantification of the percentage of Mf20 positive nuclei (**B**) and the percentage of myotubes containing more than 3 nuclei (**C**) detected by immunostaining in differentiated DM1 myoblasts for 8 days treated or not with 50 nM of digoxin for 7 days. Differentiated WT myoblasts were used as a positive control. Data represent mean± SD (n=3). **D-** Representative images of automated image acquisition and analysis on differentiate WT and DM1 myoblasts. Hoechst staining is used for software-based identification of nuclei and the area is quantified. Mf20 marker is then analyzed and area of Mf20 staining is quantified. Myoblasts were differentiated for 8 days. DM1 differentiated myoblasts were treated or not with 50 nM of digoxin for 7 days (Scale bar = 100 μm).

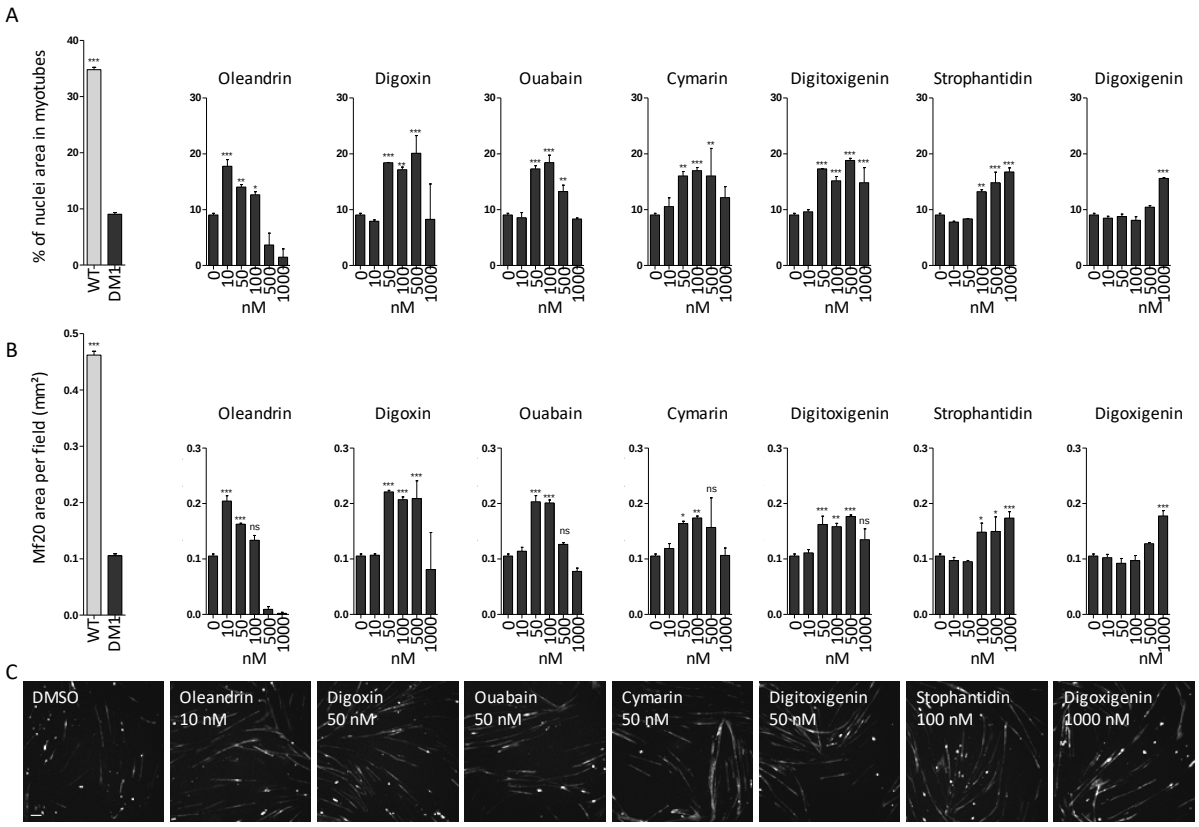

Supplementary Figure 7: Functional rescue of the in vitro myogenic impairment observed in DM1 after pulse treatment with seven cardiac glycosides, Related to Figure 7.

A-B- Dose response analysis of the effect of seven cardiac glycosides on the in vitro myogenic impairment observed with DM1 myoblasts. Automated quantification for the percent of Mf20 positive nuclei (A) and measurement of the total Mf20 area per field (B) were performed after a two days pulse treatment from day 1 to day 3 of myogenic differentiation. Myotube formation was analyzed at day 8 of differentiation. Data represent mean ± SD (n=2 experiments) and were analyzed with one way ANOVA followed by a Bonferroni post hoc test versus DMSO treated cells. *: p-value < 0.05. **: p-value < 0.01. ***: p-value < 0.00. **C-** Representative images of immunostaining for Mf20 after two days pulse treatment with the different cardiac glycosides (Scale Bar=100mm).

Table S2: List of the primers used in the study, related to Figure 2, Figure 3, Figure 4, Figure 5, Figure 6 and Figure 7

Human genes

gene	R/F	Nucleotide sequence	Technologie	Probe sequence	exon
INSR	F	GGATTACCTGCACAACGTGGTT	TaqMAN	5'-CGAGGACCCTAGGCC-3'	11-12
	R	ACGGCCACCGTCACATTC			
	F	GGATTACCTGCACAACGTGGTT		5'-CGTCCCCAGGCCAT-3'	10-12
	R	ACGGCCACCGTCACATTC			
NMDAR1	F	CGACCAACTGTCCTATGACAACA	TaqMAN	5'-CGCGGACCCAAGG-3'	exon5
	R	GGTCAAACTGCAGCACCTTCT			
	F	TGGAGGAGCGTGAGTCCAA		5'-CAGAGAAGGTGCTGCAG-3'	total
	R	AGGGCCGTCACGTTCTTG			
18S	F	Hs99999901_s1 assay in VIC-MGB	TaqMAN	Thermofisher	expression level
	R				
SERCA1	F	GCTCATGGTCCTCAAGATCTCAC	Agilent DNA 1000		+/- exon 22
	R	GGGTCAGTGCCTCAGCTTTG			
CLC1N	F	GGTCCCTTTGTTCACATCGCCAGC	Agilent DNA 1000		+/- exon 7a
mini gene	R	CTCCAAGTGGTGTTCCAAAACAGC			
cTNT	F	AGGTGCTGCCGCCGGGCGGTGGCTG	Agilent DNA 1000		+/- exon 5
mini gene	R	CATTCACCACATTGGTGTGC			
DMD	F	TTA GAG GAG GTG ATG GAG CA	Agilent DNA 1000		+/- exon 78
	R	GAT ACT AAG GAC TCC ATC GC			
MBNL1	F	GCTGCCCAATACCAGGTCAAC	Agilent DNA 1000		+/- exon 7
	R	TGGTGGGAGAAATGCTGTATGC			
MBNL2	F	ACACTTGCAGGCCAAAATC	Agilent DNA 1000		+/- exon 8
	R	CTGCTGGTAGTGCAAGACG			
DMD	F	TTAGAGGAGGTGATGGAGCA	Agilent DNA 1000		+/- exon 78
	R	GATACTAAGGACTCCCATCGC			
NFIX	F	TCGATGACAGTGAGATGGAG	Agilent DNA 1000		+/- exon 9
	R	CACAAACTCCTTCAGTGAGTCC			
UBAP2L	F	TTCATTCCGGTACTCCTGCT	Agilent DNA 1000		+/- exon 30
	R	TCCATAGTTTCCAGGCTGAG			
NCOR2	F	TGGGACGGAGATCTTCAA	Agilent DNA 1000		+/- exon 47
	R	CGAGTGCACTGAGGAGACA			
PHKA1	F	CTGGAATCTGGCAACTGGAT	Agilent DNA 1000		+/- exon 19
	R	GGGGATGAGGTGAATCAAGT			
TPM1	F	GTCATCATTGAGAGCGACCT	Agilent DNA 1000		+/- exon 8
	R	CCAGTGACTTCAAGTTGTTCG			
FN1	F	GGCCTGGAGTACAATGTCAG	Agilent DNA 1000		+/- exon 25
	R	AATGTTGGTGAATCGCAGGT			
Srp20	F	ATGCATCGTGATTCCG	SYBER GREEN		expression level
	R	CTGCGACGAGGTGGAGG			
Tra2 β	F	CGTTCCAGATCAAAGTCCAG	SYBER GREEN		expression level
	R	ATAATCTGACTGTAAGACCTG			
MBNL1	F	TTGCAAATTCAGCTGTGAGG	SYBER GREEN		expression level
	R	CGAATTTCCAAGCTGCTTTC			
CUG-BP1	F	CCTACTCGGGTATCCAGCAA	SYBER GREEN		expression level
	R	AGACACGACATTCCCAAAGG			
DMPK	F	CCAGAGCAGGGGGTCATG	SYBER GREEN		expression level
	R	CGGGCCGTCCGTGTT			
Cyclo	F	CCCACCGTGTTCTTCGACAT	SYBER GREEN		expression level
	R	CCAGTGCTCAGAGCACGAAA			

Mouse genes

Mbnl1	F	GCTGGCCAATACGAGGTCAAC	Agilent DNA 1000		+/- exon 7
	R	TGGTGGGAGAAATGCTGTATGC			
Ldb3	F	GGAACATGAGGCTCATGAGTGG	Agilent DNA 1000		+/- exon 11
	R	TGCTGACAGTGGTAGTGCTCTTC			
Clcn1	F	CTTTGTAGCCAAGGTG	Agilent DNA 1000		+/- exon 7a
	R	ACGGAACACAAAGGCACTGA			
HSA	F	Mm00808218_g1 in VIC-MGB	TaqMAN	Thermofisher	
	R				
18S	F	Mm04277571_s1 in VIC-MG	TaqMAN	Thermofisher	
	R				

Table S3: List of the Antibodies used in the study, related to Figure 6 and Figure 7

Primary Antibodies	Target	Concentration	Source
Anti-MBNL1 (Dr. Glenn Morris)	MBNL1	1/10000	Dr. Glenn Morris
Anti-CUG-BP1 antibody [HL 1190 (3B1-3D11)] (*ab50035*)	CUGBP1	1/7000	Sigma-Aldrich
Anti-Lamin A/C, MAB3211	LAMIN A/C	1/200	Millipore
Phospho-Akt (Ser473) Antibody #9271	P-AKT (Ser473)	1/1000	Cell signaling technology
Akt (Total) Antibody #9271	AKT Total	1/1000	Cell signaling technology
Phospho-GSK-3α/β (Ser21/9) Antibody #9331	P-GSK3 α/β (Ser9/21)	1/1000	Cell signaling technology
Phospho-S6 Ribosomal Protein (Ser235/236) Antibody #2211	P-rpS6 (Ser235/236)	1/1000	Cell signaling technology
S6 Ribosomal Protein (5G10) Rabbit mAb #2217	rpS6 (Total)	1/1000	Cell signaling technology
Monoclonal Anti-β-Actin–Peroxidase antibody produced in mouse, clone AC-15	Actin	1/50000	Sigma-Aldrich
Phospho-p44/42 MAPK (Erk1/2) (Thr202/Tyr204) Antibody #9101	P-ERK1/2	1/1000	Cell signaling technology
p44/42 MAPK (Erk1/2) Antibody #9102	ERK1/2	1/1000	Cell signaling technology
H3 pan (ab25631)	H3 Pan	1/1000	Millipore
Anti-SRP20 (Clone 7b4)	SRP20	1/250	Millipore
Anti-TRA2b (Clone 7a1)	SRSF10	1/250	Sigma-Aldrich
Secondary Antibodies/Isotype control	Target	Concentration	Source
ECL Anti-Mouse IgG HorseRadish Peroxidase-Linked whole antibody (from sheep)	Mouse IgG	1/10000	GE Healthcare
ECL Anti-Rabbit IgG HorseRadish Peroxidase-Linked whole antibody (from donkey)	Rabbit IgG	1/10000	GE Healthcare
Goat anti Mouse Alexa Fluor 488	Mouse IgG	1/10000	Invitrogen (Alexafluor)
Goat anti Mouse Alexa Fluor 555	Mouse IgG	1/10000	Invitrogen (Alexafluor)
Goat anti Rabbit Alexa Fluor 555	Rabbit IgG	1/10000	Invitrogen (Alexafluor)
Goat anti Rabbit Alexa Fluor 488	Rabbit IgG	1/10000	Invitrogen (Alexafluor)